Comparative metabolomics of fungal foliar endophytes and their long-lived host Astrocaryum sciophilum: a model for exploring the chemodiversity of host-microbe interactions

Leonie Pellissier, Arnaud Gaudry, Salomé Vilette, Nicole Lecoultre, Adriano Rutz, Pierre-Marie Allard, Laurence Marcourt, Emerson Ferreira Queiroz, Jérôme Chave, Véronique Eparvier, et al.

Comparative metabolomics of fungal foliar endophytes and their long-lived host *Astrocaryum sciophilum*: a model for exploring the chemodiversity of host-microbe interactions.

Leonie Pellissier[1,2]*, Arnaud Gaudry[1,2], Salomé Vilette[1,2], Nicole Lecoultre[3], Adriano Rutz[1,2], Pierre-Marie Allard[1,2,4], Laurence Marcourt[1,2], Emerson Ferreira Queiroz[1,2], Jérôme Chave[5], Véronique Eparvier[6], Didier Stien[7], Katia Gindro[3], Jean-Luc Wolfender[1,2]*

1 School of Pharmaceutical Sciences, University of Geneva, CMU - Rue Michel-Servet 1, CH-1206 Geneva, Switzerland
2 Institute of Pharmaceutical Sciences of Western Switzerland, University of Geneva, CMU - Rue Michel Servet 1, CH-1206 Geneva, Switzerland
3 Mycology group, Research Department Plant Protection, Agroscope, Route de Duillier 50, 1260 Nyon, Switzerland;
4 Department of Biology, University of Fribourg, 1700 Fribourg, Switzerland
5 Laboratoire Evolution et diversité Biologique (UMR 5174), CNRS, UT3, IRD, Université Toulouse 3, 118 route de Narbonne, 31062 Toulouse, France;
6 Université Paris-Saclay, CNRS, Institut de Chimie des Substances Naturelles, UPR 2301, 91198 Gif-sur-Yvette, France;
7 Sorbonne Université, CNRS, Laboratoire de Biodiversité et Biotechnologie Microbiennes, LBBM, Observatoire Océanologique, 66650 Banyuls-Sur-Mer, France;

*** Correspondence:**

Léonie PELLISSIER

lpellissier@invaio.com

Jean-Luc WOLFENDER

Jean-Luc.Wolfender@unige.ch

Abstract

In contrast to the dynamics observed in plant/pathogen interactions, endophytic fungi have the capacity to establish enduring associations within their hosts, leading to the development of a mutually beneficial relationship that relies on specialized chemical interactions. Research indicates that the presence of endophytic fungi has the ability to significantly modify the chemical makeup of the host organism. Our hypothesis proposes the existence of a reciprocal exchange of chemical signals between plants and fungi, facilitated by specialized chemical processes that could potentially manifest within the tissues of the host. This research aimed to

precisely quantify the portion of the cumulative fungal endophytic community's metabolome detectable within host leaves, and tentatively evaluate its relevance to the host-endophyte interplay. The understory palm *Astrocaryum sciophilum* (Miq.) Pulle was used as a interesting host plant because of its notable resilience and prolonged life cycle, in a tropical ecosystem. Using advanced metabolome characterization, including UHPLC-HRMS/MS and molecular networking, the study explored enriched metabolomes of both host leaves and 15 endophytic fungi. The intention was to capture a metabolomic "snapshot" of both host and endophytic community, to achieve a thorough and detailed analysis. This approach yielded an extended MS-based molecular network, integrating diverse metadata for identifying host- and endophyte-derived metabolites. The exploration of such data (>24000 features in positive ionization mode) enabled effective metabolome comparison, yielding insights into cultivable endophyte chemodiversity and occurrence of common metabolites between the holobiont and its fungal communities. Surprisingly, a minor subset of features overlapped between host leaf and fungal samples despite significant plant metabolome enrichment. This indicated that fungal metabolic signatures produced in vitro remain sparingly detectable in the leaf. Several classes of primary metabolites were possibly shared. Specific fungal metabolites and/or compounds of their chemical classes were only occasionally discernible in the leaf, highlighting endophytes partial contribution to the overall holobiont metabolome. To our knowledge, the metabolomic study of a plant host and its microbiome has rarely been performed in such a comprehensive manner. The general analytical strategy proposed in this paper seems well-adapted for any study in the field of microbial- or microbiome-related MS and can be applied to most host-microbe interactions.

Keywords: Endophyte; Fungi; Metabolomics; Molecular network; Metabolite annotation; Plant-Fungi interactions; *Astrocaryum sciophilum*

Introduction

It is now established that plants are not strictly distinct entities, but have rather evolved in association with highly complex and diverse microbial assemblages (Bonneville et al., 2020). These plant microbial symbiont communities (microbiota) and their collective genetic material constitute the plant microbiome (Turner et al., 2013). The plant microbiome is thought to play key roles in plant ecology and physiology, including plant fitness (growth and survival) (Dastogeer et al., 2020). It appears indeed that members of the microbiota play a role in regulating the immune system of the host plant by producing a wide range of metabolites that serve as signals involved in defense and competition, but also in interactions and communication with the host plant (Brader et al., 2014; Vorholt et al., 2017). In return, the host plant will also produce specialized metabolites to respond to symbiont colonization (Zhi-lin et al., 2007). Most signals are of chemical nature and are mediated by lipids, peptides, polysaccharides and volatile metabolites (Leach et al., 2017). Because of its ability to influence plant health and productivity and its potential impact in various applications (agriculture, drug discovery, etc.) the plant microbiome has received a great deal of attention in recent years within the scientific community. The plant that hosts a community is defined as an "holobiont". This concept considers the multicellular host and its associated microbiota as a functional entity, in which evolutionary selection probably occurs between host and microbes, but also between microbes (Rosenberg and Zilber-Rosenberg, 2016).

In this paper, we focus on fungi that reside within plant tissues, namely, endophytic fungi. The evolution of symbioses is thought to be a key event that led to the territorializing of plants about 460 million years ago (Martin et al., 2017). In particular, foliar fungal endophytes are ubiquitous and appear to influence the fitness of their host (U'Ren et al., 2019). They have been extensively studied in the last decades for their ability to produce bioactive molecules as part of a defense response against pathogens for the host or for the fungi themselves (Christian et al., 2020). Unlike in plant/pathogens interactions, endophytes can live a long time within their host, thus establishing a two-sided stable relationship involving interaction through specialized chemistry (Ludwig-Müller, 2015). Studies suggest that the host chemical profile is altered by the presence endophytes, and that host chemistry influences the composition and specificity of endophytic communities (Arnold et al., 2003).

The endophytes can influence host metabolism and induce the biosynthesis of some specialized metabolites in the host. Some fungal endophytes were for instance documented to induce the jasmonic acid and ethylene systemic defense response in plant (Van Wees et al., 2008). It is also well documented now that the endophyte and host can share parts of a particular metabolic pathway and produce a set of shared metabolites from similar precursors (Ludwig-Müller, 2015). The potential of endophytes to produce specialized metabolites that are also biosynthesized by their host plant has been a major topic of interest in the recent years. Examples include the microbial production of compounds with anticancer activities such as paclitaxel and other taxanes (Stierle et al., 1993; Zhou et al., 2010) by a wide variety of endophytic species. One possible scenario explaining the ability of endophytes to synthesize plant-associated metabolites is that homologous gene clusters present in microbes and plants could be cross-activated by metabolites produced by stress, either form the host plant or the endophytes (Howitz and Sinclair, 2008) or that genetic recombination, such as horizontal gene transfer, allows endophytes to obtain genes encoding host biosynthetic enzymes (Tan and Zou, 2001; Tiwari and Bae, 2020). Endophyte are also capable of metabolizing host products (Glenn et al., 2001; Estrada et al., 2013; Ludwig-Müller, 2015). It seems clear that the specialized chemistry of the host is shaped by both that produced by the host and that coming from the endophytes, potentially creating a protective heterogeneous chemical composition in the plant (Vega and Blackwell, 2005). Conversely, the host can influence the endophyte metabolism and shape the microbiome composition (Hansson et al., 2014). Plant can for example mimic fungal pheromones oxylipins to regulate the development of fungi, the production of mycotoxins or the attraction to insect pollinators (Gao and Kolomiets, 2009).

Given the involvement of chemistry in both the contribution of endophytes to host plant health and phenotype, and in shaping of microbial communities, it becomes particularly relevant to conduct in-depth research on the chemical links between plants and endophytes (Vorholt et al., 2017). This would assist the discovery and production of natural products of interest and unravel the potential of host-endophyte interplay. One of the main challenges is to understand the origin of a given metabolite, and to differentiate whether it comes from the plant or its inhabitants, from both or from the interaction between the two (Castro-Moretti et al., 2020).

In the context of the plant microbiota, much work has been done on endophytes to understand their ecological role and their ability to produce specialized metabolites (Lucaciu et al., 2019). The exploration of molecular and signaling mechanisms involved in plant-endophyte interactions has begun more recently, with the use of model-plant such as *Arabidopsis thaliana* (Kusari et al., 2013). There are still few studies that target a host and its community to evaluate whether the chemical production of the endophyte differs when it is isolated or in the host plant, and to what extent endophyte-derived compounds contribute to the overall specialized chemical profile of the host. Despite recent research progress, notably in omics approaches, the chemical mechanisms involved in the plant-endophyte interplay remain unclear and data are still limited (Wani et al., 2015). This may be partly because those relationships are very complex; studying *in planta* phenomena from *in vitro* living conditions is limitative, and the lack of high-quality chemical reference resources available.

The recent emergence of high-throughput sequencing and meta-omics strategies such as metagenomics and metatranscriptomics has provided a significant improvement in exploring genes, transcripts, or proteins from millions of microbes and also makes it possible to analyze biochemical functions and interactions of the microbiome with the host (Subudhi et al., 2019). In particular, next generation high-throughput sequencing techniques help collecting data on the genetic composition of microbial communities from diverse hosts and the relative phylogenetic groupings, enabling the determination of plant-microbe associations at large community level (Epp et al., 2012; Donald et al., 2020). Metabolomic analysis provides information on the metabolites sometimes numbering in the thousands of compounds and can provide a "snapshot" of metabolite production (Castro-Moretti et al., 2020).

Untargeted UHPLC-MS/MS has become one of the methods of choice for this type of analysis, as it allows to detect a wide range of metabolites with high sensitivity while providing structural insight. With the latest advances, an increasing number of unique molecules can be detected, even down to signaling molecules (Van Dam and Bouwmeester, 2016), facilitating the detection and annotation of a larger number of metabolites secreted by plants and their associated microbes (Draper et al., 2011). Recent innovations in analytical chemistry and bioinformatics are addressing the challenge of annotating and studying relevant compounds from the huge datasets produced by these techniques, including annotation of unknown compounds (Allard et al., 2016). Approaches such as molecular networking (MN) allow untargeted MS/MS data to be organized based on their spectral

similarity and thus should allow analytes to be grouped by chemical similarity. In particular, it makes comparison of metabolome composition between a wide range of samples possible, even for those in which few metabolites can be identified (Wang et al., 2016).

In this study, we aim to use these techniques to take a metabolomic snapshot of a leaf and its fungal community and study at a given time, this plant-fungal interaction from a molecular point-of-view. We used *Astrocaryum sciophilum* (Miq.) Pulle as a host plant model (Kahn, 2008). This understory palm is endemic of the northeast region of the Amazon and is particularly known for its remarkable long-life cycle and resistance (Charles-Dominique et al., 2003). Its maturation age of about 170 years and leaves up to 20 years old suggest that this palm can maintain a stable association with microbial communities over a substantial period of time. This implies that potential endophytes are able to survive and resist the environment of the plant, likely by developing interesting chemical strategies (Arnold et al., 2003). We hypothesized that reciprocal chemical interactions occur between plant and endophytic fungi, via specialized metabolites potentially expressed in host tissues.

We propose an exploratory strategy using UHPLC-HRMS/MS profiling combined with molecular networking (MN) and state-of-the-art annotation techniques to investigate the metabolome of the host leaf in parallel with the cumulative metabolome of its cultivable fungal
endophytes. Our goal was to understand the proportion and the origin of common compounds and to illustrate how both the host and the endophyte community contribute to the richness of the metabolism of the holobiont.

Results

1. Experimental design

Our study aimed to comprehensively explore the metabolome of the *A. sciophilum* leaf (host) and its endophytic fungal community, with the objective of conducting a thorough comparison. The primary goal was to identify common characteristics and potential chemical traits within the community that can be detected in the host.
Throughout this study, as mentioned in the introduction, it has to be considered that, since *A. sciophilum* is studied in his natural habitat, all the metabolomic analysis of the entire leaf

corresponds to what has been defined as the holobiont (host leaf and associated microbes). To ensure clarity in the presentation of our findings, we will refer to the "host" to represent the plant leaf tissue and the "community" to represent the fungal strains isolated from the "host".

The experiments were designed in order to explore the metabolomic data both on the fungal community and the host side, and to establish links between all the detected mass spectrometric features. The full metabolome dataset was then investigated to determine the extent of overlaps between both datasets, first at the level of all detected features, and then by considering the identity of the metabolites involved. The general workflow is summarized in Figure 1. Each step is detailed in the *Materials and methods section.*

To obtain the dataset on the fungal community, 15 cultivable strains were isolated as the leaf endopyhtes of *A. sciophilum* (Fig. 1A). Each strain was then individually cultured on solid media and extracted with ethyl acetate (EtOAc) to yield 30 enriched extracts (Fig. 1B).

To obtain the dataset on the host plant, the leaves of *A. sciophilum* were dried and extracted under similar conditions. Since it was expected that possible endophyte metabolites levels would be low, a strategy was designed to fractionate the extract at the preparative level and analyze all the enriched fractions. To this end, the crude EtOAc extract was fractionated in one step using MPLC, yielding 47 enriched fractions (Fig. 1A,C).
To obtain a detailed view of the metabolomes of the fungal endophytic community and the host leaf (through the cumulative metabolite profiles of all the fractions and the crude extract), all samples were profiled using data-dependent UHPLC-HRMS/MS (Fig. 1D).
To ensure reproducibility, all samples were acquired in triplicates, in a single series of analyses and great care was taken to avoid any possible cross-interferences. For the general datamining, only features detected in at least all replicates of a given sample were considered.

A uniform peak picking via MZmine (Pluskal et al., 2010) on all the 234 samples (30 fungal and 48 leaf samples in analytical triplicates) allowed the creation of a unique feature list (**general dataset**) of 24096 features in positive ionization mode (PI) and 10792 in negative ionization mode (NI) (Fig. 1E). In a first instance, the feature list of all fungal samples on one side and the feature list of all host-leaf fractions and extract on the other, were considered for data processing and organized as two molecular networks (MN1 and MN2) (Fig. 1F). (Fungal community metabolome (**fungal dataset**): 11072 features in PI (5982 in NI), host-leaf

metabolome (**host dataset**): 13884 features in PI (5503 in NI)). We focused mostly on PI data in this study since, at present, chemical class and in silico algorithms available for MS/MS spectral prediction are mostly efficient for this ionization mode and, overall, most of the features were detected in PI. The mass spectrometry data were deposited on the MassIVE public repository n° MSV000088516.
Both datasets were then used in a combined MN (MN3) representing the whole dataset to evaluate the number of metabolites shared and/or expressed in the fungal community and the host (Fig. 1G). All the steps and tools used for the MN creation are detailed in the *Materials and methods section.*

Most of the features showing overlap between the fungi (specific to single strains or shared by multiple strains) and the host were investigated in more depth for annotation (Fig. 1H).
Metabolite annotation was made at the chemical class level using CANOPUS in a first instance (Dührkop et al., 2021). This tool is independent from any database search and provides structural data, at the chemical class level, even for unknown compounds. This approach permitted to give a class annotation to all nodes within the general dataset and keep this information in both fungal and host datasets. Further compound-specific annotation was done considering taxonomic information and MN cluster consistency (see *Materials and methods section).* Concomittent analysis of standards and previously isolated molecules validated some annotations, that were propagated from features to features within a cluster.

A summary description of the main features of the fungal dataset is made in *Section 2*. Similarly, the major families of compounds of the host-leaf enriched metabolome are discussed in *Section 3*. Finally, the annotated features common between the fungal and the host dataset are discussed in depth in *Section 4* at the level of each individual feature.

2. Metabolome data on all cultivable strains of the fungal community

To obtain the dataset on the fungal community, several fragments of fresh leaves of *A. sciophilum* were surface-sterilized, placed and cultivated on individual Petri dishes. This enabled to isolate and identify 15 individual strains that were cultured on solid media on the small scale (Fig. 1A). The species identified for those strains are listed, per strain number in Table S1. The isolation yielded 1 Mucoromycota and 14 Ascomycota, among which 11 Sordariomycetes and 3 Dothideomycetes. The composition of this community reflects the

taxonomic trends that have been observed in foliar endophytic fungal communities. Indeed, Dothideomycetes and Sordariomycetes represent the majority of foliar endophyte species and account for 75 % of the endophytes isolated around the globe (Arnold, 2007). The genera include those commonly isolated from tropical trees, as illustrated in (Roy and Banerjee, 2018), namely *Colletrotrichum* Corda, *Curvularia* Boedijn, *Pestialotiopsis* Steavaert and *Fusarium* Link. This indicated that the sampled foliar endophytic fungal community is representative to what is generally encountered in the natural ecosystem.

Individual strains were extracted with EtOAc to yield 30 enriched extracts and analysed according to the generic metabolite profiling method detailed in the experimental design (see *Materials and methods section*) (Fig. 1B, D). The MN corresponding to the fungal dataset (MN1) for PI data permitted grouping 11072 spectra in 6924 clusters (5982 spectra in 2755 clusters in NI).

The first annotation step with CANOPUS enabled to get a global overview of the compound classes measured in the fungal samples. In Figure 2A, the chemical pathway repartition was color-mapped on the MN and this highlighted the structural type for each node (Fig. S1A). The main chemical classes are represented as a hierarchical sunburst diagram. Each NPclassifier category was assigned to a circle area, with their subcategory circles nested inside while the number of associated features for each category are displayed via area size. The innermost circle is as the top of hierarchy. A detailed and interactive view of the sunburst diagrams is available at Interactiveplots. Overall, CANOPUS enabled the chemical class annotation of 4268 features out of 11072 with the following percentage repartition at the pathway level: 39.5 % fatty acids, 17.0 % terpenoids, 13.5 % polyketides, 13.0 % amino acids and peptides, 8.5 % shikimates and phenylpropanoids, 7.5 % alkaloids, 2.0 % carbohydrates.

The processing of all the information in the MN allowed to highlight features shared between two or more strains and to interpret these compositional overlaps. Annotations of features confirmed by a standard or an isolated molecule are highlighted with a star (⁎). The taxonomical information was also represented by colors on the MN (one color for one strain, shades of the same color for different strains of the same genus) to have an overview of the strain of origin for each node (Fig. 3).

To evaluate the major trends in the dataset, the metabolite chemical classes shared between few endophytic species were identified. In practice, to assess overlap rates, individual features detected in more than three samples from different species, *i.e.*, nodes tagged with 3 or more colors (one color corresponds to one species) were examined. For example, the feature that corresponded to 24(28)-dehydroergosterol was shared by 7 species and highlighted in cluster Fig. 3_1a. Most of the features of the associated cluster were annotated as ergostane steroids by CANOPUS, and were also shared by multiple species (Fig. 3_1).

Common classes of metabolites were also highlighted when specific features were not shared between samples but linked through a shared cluster (nodes having one color only, grouped with nodes of another color). This indicated that they have common substructures leading to spectral similarities and thus potentially common biosynthetic pathways. This is illustrated in cluster Fig. 3_2, mostly annotated as glycosphingolipids. Other clusters displaying common fungal metabolites classes are shown in Fig. S2. Those corresponded mostly to glycerolipids (Fig. S2_1) (Griffin, 1996), purine nucleosides (Fig. S2_2) (Moffatt and Ashihara, 2002), amino acids and peptides derivatives including cyclic peptides (Fig. S2_3) (Wang et al., 2017), dipeptides (cluster 17, Fig. S2_4-5) (Mishra et al., 2017), polyketides (Fig. S2_6) and shikimates and phenylpropanoid derivatives (Fig. S2_7) (Tzin et al., 2012; Cox et al., 2018). Overall, these annotations make sense with respect to what is known for fungal metabolites (Zhang et al., 2006). The occurrence of such compounds in most of the species was expected, as ergostane steroids are sterol specifically found in fungal cell walls (Nes et al., 1989; Klemptner et al., 2014) and glycosphingolipids are ubiquitous component of the fungal membrane (Fernandes et al., 2018).

Clusters and features found to be specific to strains and/or particular species could also be evidenced (clusters containing mostly single-color nodes). For instance, the cluster in Fig. 3_3 containing nodes coming principally from *Fusarium concolor* Reinking (taxon synonym *Fusarium polyphialidicum*) strains (A4, A6) and most of the nodes were annotated as compounds from the 3-decalinoyltetramic acids class (superclass: cyclic polyketides). Within this cluster, for example, the feature at *m/z* 374.232, t_R 4.83 (molecular formula $C_{22}H_{31}NO_4$) was annotated as equisetin by SIRIUS and fully identified by the injection of a standard. This is consistent since this compound and its derivatives have already been specifically isolated from *Fusarium* sp. (Sims et al., 2005). Other examples include a cluster specific to *Curvularia* sp. strains (A3 and A14) (Fig. 3_4) were the features were annotated as cytochalasan alkaloids metabolites. Within this cluster, the feature at *m/z* 480.274, t_R 2.99

was annotated by SIRIUS as cytochalasin B and the annotation was confirmed by the injection of a standard. This is well in line with previous reports indicating the occurrence of cytochalasin A or B in *Curvularia* sp. (Khiralla et al., 2019). Additionnal specific clusters were evidenced and highlighted (Fig. S2_8-15): jasmonates derivatives (Fig. S2_8) and naphtalenes polyketides (Fig. S2_15) in *Lasiodiplodia* sp. (Salvatore et al., 2020), shikimates and phenylpropanoid (coumarins, isocoumarins) in *Diaporthe* sp. (Luo et al., 2018) (Fig. S2_9), azaphilones in *Trichoderma lentiforme* (Pang et al., 2020) (Fig. S2_10), histidine alkaloids in *Fusarium* sp. (Wen et al., 2015; Ma et al., 2022) (Fig. S2_11-12). Overall, the annotation results proved to be consistent with literature data on the corresponding fungal species or genera, even before taxonomical re-ranking.

Altogether, analyses on the dataset reveal a consistent chemical class annotation for ubiquitous fungal compounds as well as at a species-specific level. Metabolite profiles also revealed a good clustering trend according to the taxonomy of the fungi. PCoA (Bray-Curtis dissimilarity metrics) and Hierarchical Cluster Analysis (HCA, single linkage method) were computed based on metabolite fingerprint (PI) of the 15 strains using the fungal-dataset feature table and showed that samples were clustered together according to their taxonomical affiliation (Fig. S3). This showed that the set was informative at the chemical level, thus enabling the exploration of data on the fungal community as such.

3. Deep metabolome data on the palm host leaf *Astrocaryum sciophilum* (holobiont)

The MN corresponding to the host dataset (MN2) (crude extract and enriched fractions) for PI data allowed to group 13884 spectra in 8315 clusters.

Using CANOPUS, the initial annotation phase allowed to obtain a comprehensive overview of the compound classes measured in the host-leaf samples, by benefiting of the enrichment procedure described in *1.4*. All the annotations have been processed the same way as for the fungal dataset, the chemical pathway repartition color-mapped on the MN and the main chemical classes represented as a hierarchical sunburst diagram (Fig. 2B, Interactiveplots). Overall, CANOPUS enabled the chemical class annotation of 5957 features out of 13884 with the following percentage pathway repartition: 36.0 % fatty acids, 35.0 % terpenoids, 12.0 % shikimates and phenylpropanoids, 8.5 % polyketides, 4.5 % alkaloids, 3.0 % amino acids and peptides, 0.9 % carbohydrates (Fig. 2B).

The chemical CANOPUS class repartition was color-mapped on the MN (Fig. S1B). The sample type (EtOAc extract or MPLC fraction) was also represented by colors (shades of green) on the MN to have an overview of the sample(s) of origin for each node (zoomed squares Fig 4). This enabled to get a global overview of the compound classes measured in the plant extract and fractions. Well represented chemical classes were highlighted: glycerolipids (Fig. 4_1-4), sphingolipids (Fig. 4_5), fatty acids and conjugates (Fig. 4_6-7), (apo)carotenoids (Fig. 4_8-9), steroids (Fig. 4_10-11) terpenoids (Fig. 4_12), triterpenoids (Fig. 4_13-14). Some chemical classes such as glycerolipids and fatty acids conjugates were also detected in the crude extract, indicating that they could be main metabolites. Some were well spread in the fractions or more specific to one fraction, such as lignans, that are detected mostly in fraction 33 (Fig. 4_15-16). Some have been reported as produced by the Arecaceae family: lanostane triterpenoids reported in *Sabal* sp. (El-Dib et al., 2004), cholestane steroids (Tapondjou et al., 2015), flavonoids (de Oliveira et al., 2013) (Fig. S4A, B, C), and even by the genus *Astrocaryum* such as carotenoids (Noronha Matos et al., 2019) (Fig. S5). Within the carotenoids in cluster Fig. 4_8, the feature at *m/z* 551.42, t_R 6.56 was annotated as β,β-caroten-4-one and annotation was confirmed by the injection of a standard.

The MN processing also allowed to visualize each feature's detection status: only in the crude extract (Fig. S6A_1), only in the fractions (one or more) (Fig. S6A_2), or in both (Fig. S6A_3). Features found only in the extract might be compounds degraded in the fractions or retained in the MPLC column. As shown in Fig. S6B, the sum of all the features detected in the fractions was much higher than the one obtained only by profiling the raw extract. Indeed, features contained in the crude EtOAc extract accounted for only 3.7 % of the total features detected (510 features detected in the crude extract, 13592 in the MPLC fractions). The enrichment process effectively unveiled about 30 times more features compared to the total crude extract profiling. These features were well-distributed across the MPLC fractions. Hence the importance of the enrichment step to improve the detection of minor compounds and shared features in the MN comparative analysis (Fig. S7).

4. Global comparison of the entire metabolome dataset: host leaf (holobiont) and foliar fungal endophytic community

In a next phase, as both UHPLC MS/MS datasets belonged to the same data table and all sample origin metadata were available for each feature, the process described for sections 2

and 3 could be applied to the whole general dataset (fungal+host). This ensured a consistent connection between all features and their corresponding annotations. Consequently, a single MN encompassing all filtered fungal and host features was created (MN3), highlighting the correlations existing among all detected features spectra (see *Materials and methods section*, MassIVE Dataset n° MSV000088516). This led to group 24096 spectra in 14473 clusters.
All features that were directly shared between the endophytes and the host were highlighted. Additionally, features associated with fungi were grouped together in clusters associated with plants, probably demonstrating links at the level of shared given classes or structural skeletons. Conversely, this approach also revealed clusters or features that were detected only in host or fungal samples.

4.1. Comparative analysis of the general dataset

A first survey of the data showed that, at the cluster level, 425 clusters were shared between the plant and the fungal community, potentially corresponding to compounds of similar chemical class. At the feature level, among the 24096 detected features in PI, about 860 (4 %) were detected both in the plant host and in the fungal community (Fig. 5A). In NI, 693 (6 %) were shared among the 10792 detected features.
If the same comparison was made only with the metabolite profiling obtained with the raw extract, this would evidence only 70 shared features (0.3 %). The significant host leaf extract enrichment process was therefore effective to reveal about 10 times more shared features (Fig. S8).
Among the shared features, each endophytic strain has revealed between 18 and 42 % of shared features with the host (150 to 500 feature by strain) (Fig. S9). Considering only the number of shared occurrences, it seemed that, among all endophytes, some strains (A2, A7, A15, A100, A14) had a metabolic signature detectable at the leaf level, while some (A8, A9, A13) had a more subtle expression. Bearing in mind possible analytical and physiological variations, this suggested that some strains were more expressive than others. This aspect should be balanced by the fact that the metabolites shared correspond to fungal specialized metabolites.

4.2. Annotation of shared features (case studies)

To conduct a thorough study, the dataset needed to focus on annotated/identified metabolites that were present in both endophytes and the host leaf.

In addition to the annotation obtained with CANOPUS (see parts *2* and *3*), a complementary annotation phase was used (ISDB with taxonomic and consensus chemical classification reweighting), focusing on PI data.
Furthermore, the use of standards and previously isolated molecules enabled to unambiguously indentify more than 40 features and help the overall annotation process through the propagation to more than 50 additional features (Fig. S10-15, Table S2).

On the 24096 features from the general dataset, the CANOPUS chemical class led to the annotation of 20314 features at the pathway level (Fig. S16A), 16156 at the superclass level (Fig. 5B), and 9808 at the class level (Fig. S16C). In the histogram display in Fig. 5B, the total number annotated features per chemical categories is indicated on the top level along with the repartition of the features in the host leaf (blue), the fungal community (orange), or both (green). Considering only the features shared between the host and the fungi, the annotations were organized as a hierarchical sunburst diagram (Fig. 5C, detailed and interactive view available at Interactiveplots). The chemical pathway annotation of the shared features was distributed as follows: 69.0 % fatty acids, 10.5 % terpenoids, 5.5 % alkaloids, 5.0 % shikimates and phenylpropanoids, 4.0 % amino acids and peptides, 3.6 % polyketides, 2.0 % carbohydrates.

The analysis of the general dataset based on the NPclassifier ontology (Kim et al., 2021) revealed that the chemical pathway that was most commonly found to be shared between plants and fungi was that of fatty acids. An overview of this data indicated that feature related to terpenes and shikimates were mostly found in the host plant leaf while amino acids and peptides derivatives were mostly detected in the fungal endophytic community. Fatty acids and polyketides were well spread between both. This trend was already reflected in the separated analysis of the host and fungal datasets (see *2* and *3*, sunbursts).
The frequency of features at each superclass level was then considered. For this, all categories regrouping more than 15 features were analyzed and specificity was assessed when more than 90 % of features were found either in the host or the fungi. For the host, the main specific superclasses were triterpenoids, apocarotenoids, diterpenes and lignans. For the fungi, they were oligopeptides, glycerophospholipids and naphthalenes. Varying percentages of shared features and also of shared clusters were observed.

To better document the host-endophyte interaction, most frequently shared features were initially analyzed category by category, taking into account what has been reported in the literature in general in plant-fungi interactions.

4.2.1. Shared features well spread between fungal and host datasets

The data indicated that most of the shared metabolites belonged to fatty acids, and the following superclasses: glycerolipids, fatty acids and conjugates, octadecanoids and steroids and more specifically at the class level, to mono-, di- and triacyclglycerols (MAG, DAG, TAG), dicarboxylic acids, unsaturated fatty acids, octadecanoids (See Interactiveplots). In a first assessment, these findings appeared logical since this type of metabolites is known to be produced by both plants and fungi. Indeed, fatty acids are ubiquitous in nature and represent a major chemical class involved in physiologically important processes such as membrane structure, energy storage and signaling pathways (Athenaki et al., 2018; He et al., 2020).

Specific features or analogues of fatty acids commonly detected in one or more of the endophytic fungi and in the host leaf were studied. Partial feature table and annotations can be found in Table S2 and the full peak list is provided in Table S3.

4.2.1.1. Shared glycerolipids

The distribution histogram shows that the most frequently shared features corresponded to glycerolipids (GL) (Fig. 5A,B, Interactiveplots, corresponding clusters Fig. 6_C1-4). This was particularly true for triacylglycerols (TAGs) and diacylglycerols (DAGs). In C1, most of the features came from the host samples, indicating that TAGs and DAGs were found abundantly in the leaves (Fig. 7). A detailed analysis of these shared features showed for example that, the feature **n3** at *m/z* 613.483, t_R 7.11 (613.483@7.11) was found in the host as well as in the strain *Colletotrichum* sp. (A16) (Fig. 7_C1_n3). This feature corresponded to the protonated molecule $[M+H]^+$ of a diacylglycerol (DAG) the of molecular formula of which was $C_{39}H_{64}O_5$ (Δppm 1.5) and was annotated as DAG (18:3n3/18:3n3) (see Table S2). The figure also shows the extracted ion chromatogram for the shared features in either the fungal strain or MPLC fraction profile. This allowed to verify that the alignment, especially in terms of retention time, was correct for the feature found to be shared. The MS/MS fragmentation patterns for the feature in the strain or in the plant were associated and compared, and allowed to ensure that the metabolite found to be shared by both samples was of the same hypothetical structure (Fig. 7_C1_n3). As an example for MAGs, cluster C4

showed that several isomers of the MAG 2-monolinolenin were shared between some fungal strains and the plant leaf (Fig. S17_C4_n1-n3_ feature **n1**, 353.2696@5.1).

The results obtained on the various MAGs, DAGs, TAGs detected is coherent since this kind of metabolites are known to be produced by both plants and fungi. GLs are part of the basic component of the animal, plant, microbial cell membranes and lipid body fractions (role in carbon storage for energy, lipid metabolism and lipid-mediated signaling pathways in plant and fungi) (Zhang et al., 2012; Lastovetsky et al., 2016; Siebers et al., 2016; Qiu et al., 2020). It is also known that GLs might have a role in the response to microbial pathogenic or beneficial invasion, going from signal reception at the host plasma membrane, to transduction and downstream defense pathway through induced or acquired systemic resistance (Siebers et al., 2016). In pathogenic interactions, DAGs could act as secondary messengers for the regulation of developmental processes, but also to modulate the lipid composition of the host membrane for colonization and invasive growth (Sadat et al., 2014). In symbiotic relationships, especially at the root level, it was demonstrated that DAGs and TAGs production was increased during arbuscular mycorrhizal formation probably to create a larger exchange surface and energy storage and also generate JA derivative during defense response. The fungal fatty acid palmitvaccenic acid stored as a TAG is in fact used as a marker of the mycorrhizal colonization (Siebers et al., 2016; Macabuhay et al., 2021). MAGs such as monolinolenins could be involved in plant defense as they have been shown to accumulate upon fungal infection and to interact with the membrane of diverse pathogenic bacteria or fungi (Kusumah et al., 2020; Toljamo et al., 2021). Overall, it is however difficult to say with this dataset if the shared specific GLs detected in leaves result from the symbiosis with the fungal strains for which we could clearly evidence these compounds when cultured *in vitro*, or if the leaf or root itself is producing them (Agostini-Costa, 2018).

4.2.1.2. Shared unsaturated fatty acids

Unsaturated fatty acids and octadecanoids were also frequently detected in both the host and the fungi. These NPclassifier categories are strongly linked and will be discussed together. Examples of corresponding clusters were evidenced in the MN (Fig. 6_C7-9).

In cluster C7, several features were classified as unsaturated fatty acids, others as octadecanoids (Fig. S18_C7_ n1-n13). Several ions corresponded to linoleic acid or isomers. Some were found to be specific to fungal strains (*Fusarium polyphialidicum* A4 and A6,

Lasiodiplodia venezuelensis A2, *Curvularia eragrostridis* A3, *Neopestalotiopsis ellipsospora* A1) (Fig. S18_C7_n1-n3) or some were detected only in the plant, and annotated as fatty acids found in Arecaceae (Fig. S18_C7_n4-n8) (de Oliveira et al., 2016; Agostini-Costa, 2018). Several of them were shared with the host: 279.2321@6.74 annotated as alpha-linoleic acid and found in *Fusarium polyphialidicum* (Fig. S18_C7_n9), or 279.2325@4.48, a potential isomer found in multiple strains including different *Fusarium* sp. strains, a *Colletotrichum* sp. Strain (Fig. S18_C7_n10; 293.2475@5.28 annotated as the methyl ester, methyl alpha-linoleate, and shared between *Fusarium decemcellulare*, *Lasiodiplodia venezuelensis* (Fig. S18_C7_n11). Similarly, octadecanoids were found in the cluster specific to the leaf and *Curvularia* or *Fusarium* strains. Such fatty acids have already been reported in *Lasiodiplodia* sp. and *Fusarium* sp. (Shahnazi et al., 2013; Salvatore et al., 2020).

In cluster C8, most of the unsaturated FA detected were annotated as methylated and oxygenated derivatives (Fig. S19), and came from the fungal strains *Curvularia eragrostridis* (A3, A14) and *L. venezulensis* (A2). Some of these features were shared with the plant leaf (Fig. S19_C8_n1-n3)). According to the literature, such derivatives have indeed been found in *Curvularia* sp. and *Lasiodiplodia* sp. (Devi et al., 2006; Salvatore et al., 2020). (10*E*,12*Z*,15*Z*)-9-Hydroxy-10,12,15-octadecatrienoic acid methyl ester (**n3**) was notably found to be a defense substance of some plants against pathogenic fungi (Dong et al., 2000).
Unsaturated FA are also ubiquitous in nature and essential components of eukaryote cell membranes (Athenaki et al., 2018; He et al., 2020). In particular, polyunsaturated fatty acids (PUFAs) are the precursors of oxylipins, their oxygenated metabolites. Oxylipins in plant serve as signal molecules mediating the responses to biotic/abiotic stresses and developmental processes. In fungi, they are also linked to basic developmental processes (spores, germination, quorum sensing, mycotoxins production) (Böttcher and Pollmann, 2009; Brodhun and Feussner, 2011).

Interestingly in the dataset, fungal oxylipins were also detected among the shared features.
Cluster C15 (Fig. 6_C15) contained several features annotated as eicosanoids (C20 PUFAs) derivatives, prostaglandins (PGs). Two of the features annotated as PGs were detected as shared between the *Fusarium decemcellulare* strain A100 and the leaf (Fig. 8_C15_n1-n2). a Additionally, a clusters of cyclic oxylipins related to jasmonic acid (JA) and derivatives could be detected as coming mostly from the *Lasiodiplodia* A2 strain (e.g. Fig. S2_C8).

Eicosanoids belong to fungal oxylipins, structurally akin to plant ones, and might be involved in signaling and regulating host immune responses, such as tolerance during the colonization. Research showed that PGs can be synthesize either *de novo* or by using the host's arachidonic acid. Certain pathogenic fungi such as *Bisifusarium dimerum* even employ prostaglandins as a virulence factor to downregulate host immunity (Noverr et al., 2003). Several fungal species such as *Fusarium oxysporum* and *Lasiodiplodia* sp., are known to secrete JA and its derivatives, that could play an important role in the host-endophyte interactions (Miersch et al., 1999; Tsukada et al., 2010). Such cyclic oxylipins, have many physiological roles in plants such as senescence, pathogen defense, signaling processes (Schaller, 2001).

Oxylipins are regarded as interkingdom communication signals because of the striking similarity between the sets of oxylipins produced by plants and fungi, especially the lipoxygenase products 9S-HPODE and 13S-HPODE.
Several studies have evidenced a "lipid language" between plants and fungi, involving PUFAs and oxylipins, which is likely to be conserved across multiple fungal species (Christensen and Kolomiets, 2011). Plant oxylipins can affect fungal secondary metabolism, while fungal oxylipins can mimic endogenous signal molecules, influencing processes in host tissues (Brodhun and Feussner, 2011). Certain plant pathogens can manipulate plant defense response by mimicking the plant hormone JA (Wasternack and Kombrink, 2010). Conversely, certain fungi respond to plant oxylipins, which in turn influence their development (Calvo et al., 1999). The manipulation of host oxylipins by fungi is thought to be involved in enhancing symbiotic relationships for example by producing elicitors to induce JA biosynthesis, boosting the host's resistance to fungal pathogens (Djonović et al., 2007).
The similarity of the metabolites potentially identified here makes it difficult to conclude that the molecules found in the plant are a remnant of the biosynthetic activity of fungi. However, since they are rather specific and detected mostly in fungal strains, their detection in the leaf could indicate the metabolic signature of these endophyte at the host level.

4.2.1.3. Shared dicarboxylic acids

The dicarboxylic acids and derivatives (FA and conjugates superclass) were particularly shared between plants and fungi. This was exemplified in cluster C10 and C11 (Fig. 6_C10-11). In C10, the features **n1** and its ammonium adduct **n2**, and **n3** were shared between multiple MPLC fractions and *Fusarium* sp. strains A15 and A100. Particularly, the feature **n3**

was putatively annotated as 4-oxo-azelaic acid (4-oxo-AZA) (Fig. 9_C10_n3). In NI, the feature at 187.0985@1.72 shared between the *Fusarium* strains A4, A15 and A100 and multiple MPLC fractions corresponded to the $[M–H]^-$ of a molecule with the MF $C_9H_{16}O_4$ and was annotated as azelaic acid. This showed that azelaic acid as well as its 4-oxo derivatives were indeed shared between plant and fungi.

Dicarboxylic acids, also produced by oxidation of unsaturated fatty acids in higher plants and mammals (Mingrone and Castagneto, 2006). The C_9 dicarboxylic acid azelaic acid (AZA) is known as a defense messenger and component of systemic acquired resistance (SAR), produced specifically after plant infection and travels through the plant via the vasculature to trigger immunity and defense signals (Jung et al., 2009). AZA, and 4-oxo-AZA were found to be accumulated in mycorrhized plants as a local response to herbivory damage in leaflet and seem to be part of the leaf metabolome reprogramming after attacks, regulated by arbuscular mycorrhizal fungi. Moreover, 4-oxo-AZA has already been isolated from a *Fusarium* sp. (Sbrebryakov et al., 1970). Its presence in the leaf might thus be the result of the *Fusarium* strains production.

4.2.2. Shared features attributable to fungal strains

Through the detailed view of the metabolites produced by the fungi (see part *2*), number of metabolites attributable to specific fungi, could be identified and checked for their occurrence in the leaf samples.

4.2.2.1. Shared steroid derivatives

Steroid derivatives were highlighted as common components both specific to plant (Fig. 4_10-11) and to fungi (Fig. 3_1). Sterols appeared in several specific clusters (Fig. 6_C12-C14) in the general MN, which seems logical since it is known that sterol biosynthesis is divergent in plant and fungi (Darnet et al., 2021). However, some features were shared, such as feature **n1** in the cluster C14 (Fig. S20_C14). The detection of sterols rather specific to fungi could be a trace of their membrane constituents and thus evidence of their occurrence in the leaf. Fungal sterols are also known to be involved in non-plant signal perception by the plant, in pathogenic as well as symbiotic interactions (Rodrigues, 2018).

4.2.2.2. Shared cytochalasan alkaloids

Cluster C17 gathers a group of cytochalasan derivatives in which the annotation of **n1** was confirmed by injection of a cytochalasin B standard and propagated (Fig. 10). Most of the

features came from the *Curvularia* strains A3 and A14 (Fig. 10_C17_n2-n6), and cytochalasin B has indeed been isolated from *Curvularia lunata* (Wakker) Boedijn (Wells et al., 1981). However, 4 associated nodes were coming from the plant. The feature **n2** at 480.2827@2.99 was detected in the plant only but corresponds most probably to an isomer of cytochalasin B. The feature **n3** was also detected in the plant only and annotated as the 7-*O*-acetyl-cytochalasin B, only known to occur in fungi (*Phoma* sp. Sacc.) (Fig. 10_C17_n3) (Capasso et al., 1991).

Cytochalasins are cell-permeable fungal metabolites (mycotoxins) also isolated from *Xylaria* sp. Hill ex Schrank, *Phomopsis* sp. (Sacc.) Sacc., or from an amazonian endophyte *Aspergillus* sp. P. Micheli ex Haller (Amaral et al., 2014; Chen et al., 2015, 2017; Feitosa et al., 2016). They have a wide range of biological activities and might be involved in the mediation of plant-fungi relationships notably through the regulation of plant growth (cytochalasin H) (Cox et al., 1983), and the regulation of fungal growth and secretion (cytochalasin A, Fig. 10_C17_n7) (Torralba et al., 1998) . Particularly, they act on cellular processes via their ability to bind actin filaments and inhibit its polymerization. By acting on the polymerization of microtubules and actin filaments, cytochalasins were found to have an impact on the outcome of the attempted penetration of non-pathogenic fungi. Kobyashi *et al*., showed that a treatment of barley coleoptile with cytochalasin A allowed non-pathogens fungi including *Gloeosporium orbiculare* (Berk.) Berk.(taxon synonym *Colletotrichum lagenarium* (Pass.) Ellis & Halst.) and *Alternaria alternate* (Fr.) Keissl. to penetrate and form haustoria in the coleoptile cells, without affecting the stability and arrangement of microtubules. In non-treated coleoptiles, the non-pathogens always failed to penetrate the plant cells (Kobayashi et al., 1997). Remarkably, the recent chemical investigation of a *Colletotrichum* sp. strain also isolated as an endophyte from *A. sciophilum*, led to the isolation of cytochalasins, proving that they most likely represent the unique chemical marker of a fungal strain in this case (Barthélémy, 2019).

These findings demonstrated that certain fungal strains, as well as the leaf itself exhibited detectable levels of cytochalasins. These compounds might have been used by certain endophytes to enter host plant's cells, their distinctive chemical signature remaining detectable even at the plant level. Beyond their antipathogenic properties, fungal cytochalasins may be present in the plant's metabolome to influence signaling pathways and facilitate interaction processes between the endophytes and their host plant.

4.2.2.3. Shared apocarotenoids

Cluster C18 was annotated as apocarotenoids ε- detected in different strains of *Fusarium*, *Curvularia*, and *Pestalotiopsis* as well as in the leaf (Fig. S21). Annotation of the feature **n1** (Fig. S21_C18_n1) as 3-hydroxy-4,7-megastigmadien-9-one was confirmed since it was isolated from the plant. Apocarotenoids are carotenoid derivatives synthesized through the enzymatic action of carotenoid cleavage dioxygenase (CCD) in plants, algae, fungi and bacteria (Nisar et al., 2015). They serve in diverse key biological processes including color and volatile attractant in plant-animal communications, and assume a significant signaling role in the interactions between plants and their environment, particularly in plant-microbial interactions (Walter et al., 2010). Some studies showed that apocarotenoid biosynthesis was triggered in roots upon symbiotic arbuscular mycorrhizal colonization, resulting in the accumulation of cyclic C_{13} and linear C_{14} apocarotenoids, such as 3-hydroxy-4,7-megastigmadien-9-one (**n1**), blumenols and mycorradicins (Fiorilli et al., 2019). They have been proposed as foliar markers of AM symbiosis due to their transport to aboveground organs via the shoots, where they also accumulate. These molecules possess a moderate, rather than overly strong antimicrobial and growth-inhibiting properties, which may enable a milder defensive response to symbionts than to pathogens (Wang et al., 2018). Several studies have provided evidence that microbes, notably endogenous fungi isolated from boronia or marigold, were able to produce C_{13} norisporenoids, including 3-hydroxy-β-ionone (similar to **n1**) via the degradation of carotenoids such as lutein facilitated by fungal enzymes (Sánchez-Contreras et al., 2000; Rodríguez-Bustamante et al., 2005; Khatri et al., 2010).
Interestingly, this study reveals that the endophytic fungi have the capability to produce these compounds even when cultivated in isolation. Clusters of fungal carotenoids potentially serving as precursors, were found in the same *Fusarium* strains (Fig. 6_C19-20) indicating that these fungi likely possess the necessary substrate for biotransformation in the culture media.

Discussion

The ability to detect common features in both fungal and host datasets, within the global metabolomic dataset, highlights the effectiveness of the workflow in generating data that allows for a comprehensive analysis of the co-occurrence of corresponding metabolites.

Overall, the findings indicate that only a small proportion of all detected features (3.7 %) were common to both host leaf and fungal samples, despite the significant enrichment achieved through plant fractionation. This suggests that at the leaf level, the presence of fungi is barely detectable through their specific metabolomic signature, obtained when the corresponding strains are cultivated. In general, the most commonly shared metabolites appear to align with those known to be produced by both fungi and plants. It is therefore difficult to say whether this is indicative of the fungal presence in the leaf. Such discrimination would only have been possible with the analysis of a cultivated leaf devoid of its endophytic community. This was not the aim of the study since its focus was on monitoring the metabolome of the palm in its natural habitat.

This observation suggests that the endophytes present in the analyzed leaf samples may be metabolically inactive or show limited metabolic activity in this specific context, particularly concerning their specialized metabolites.

Nonetheless, as discussed, the subset of shared metabolites may be involved in an interplay between the organisms (e.g. for signaling, infection establishment, and immune response). Several of these metabolites were previously recognized as markers of fungal symbioses, particularly in plant roots, and our analysis reaffirms their significance in this context.

Research findings revealed that some metabolites and their associated gene expression increase upon endophyte presence and are linked to plant defense responses (oxylipins, unsaturated fatty acids, JA) and corroborate some of our results (Mejía et al., 2014).

As discussed above, oxylipins play a part in inter-kingdom cross-talk and might be involved in host-fungal communication due to their structural similarity between plant and fungal components (Christensen and Kolomiets, 2011). Fatty acids can be used by endophytes to influence the chemical and physical properties of the leaf membranes, and in turn enhance the host's robustness and resistance to pathogens while also reducing the herbivores appetence. Producing or modifying such metabolites can also be involved in the recognition establishment of partner endophytes. For instance, cytochalasins could aid in colonization (Kobayashi et al., 1997), while GLs may contribute to differential recognition between symbionts and pathogens (Siebers et al., 2016).

Endophytes produce metabolites or induce in the host the production of metabolites that are also directly involved in outcompeting undesired or pathogenic microbes by activating the plant's immune and defense response, through for example bioactive polyketides or

sesquiterpenes or, as discussed, dicarboxylic acids such as AZA and its derivatives (Mattoo and Nonzom, 2021).

On the other hand, prostaglandins can function as signal molecules to downregulate host immunity and the presence of fungi in the host. The biosynthesis of metabolites such as C13 isoprenoids with moderate antipathogenic activity may allow for milder defensive measures towards other symbiotic organisms. Ultimately, metabolites produced by both the host and endophytes play a crucial role in facilitating fungal colonization and shaping endophyte communities. They allow endophytes to maintain asymptomatical growth while maintaining a balanced antagonism with the host and other constituents of the microbiome (Schulz and Boyle, 2005). This delicate interplay of metabolites allows for a nuanced and dynamic interaction between the host and various symbionts, ensuring a finely tuned coexistence and the health and functionality of the ecosystem.

Despite employing a consequent enrichment process, the detection of traces of specific metabolites *in folio* that were expressed *in vitro* proved to be challenging. This may be because these metabolites are not present in the leaf at all, or exist in quantities that are below the detection limit of the analytical approach. They might also have a highly localized distribution within the leaf (Arnold et al., 2003), and be interwined with a vast array of plant metabolites, creating interferences hampering their detection.

Another plausible explanation could be that metabolite production is low when the fungi reside inside the leaf. Our previous studies have shown that potential endophyte communities in *A. sciophilum* appear to be uncompetitive. This was evidenced by to the lack of antipathogen activity *in vitro* and also through co-occurrence metagenomic studies (Donald et al., 2019). It could be assumed that this endophytic community of “old leaves” has established a balanced environment with its host, and might be metabolically “static” or not highly active, in contrast with a community constantly encountering host or exterior defense chemicals (Arnold et al., 2003).

Since some of the specific fungal metabolites and shared metabolites are however detectable in the holobiont, it can be concluded that the endophyte community at least partly does contribute to its metabolome. This does not prevent a contribution to a possible better fitness of the plant. Indeed, a product present in small quantities can have a major biological role in the plant. However, the chosen model (slow-growing palm in its natural environment) does not allow a clearer statement. As mentioned, studies involving plant material produced under

perfectly sterile conditions would be necessary to more specifically assess the metabolome contribution of each endophytic fungus.

It must be recognized that the application of an untargeted metabolomic approach to the study of a complete holobiont remains extremely challenging, even after an extensive metabolite enrichment at the host level. An even more accurate detection of the endophyte/host interplay at the molecular level may require more sensitive and/or more targeted methods. Furthermore, it has to be kept in mind that this represent only a part of the fungal endophytes and other endophytes not cultivable *in vitro* have been missed.
Such study could be complemented by using different models (other origins, different developmental stage) in which we could use traceable systems, target the producing organs, or work on differential inoculation in the host. Combinations of data with other omics tools (metagenomics, transcriptomics) to study the associated biosynthetic genes for instance would clearly help in understanding the underlying mechanisms involved in symbiosis (Lucaciu et al., 2019).

Our study provides a deep metabolome survey of a long-lived holobiont in its natural habitat. It contributes to extend the knowledge about the possible chemical interactions related to the symbiosis between the endophytic fungal community and the host using an advanced untargeted metabolomics workflow. The proposed approach can be adapted to the investigation of other host-microbe interactions. The results obtained shade light on how such challenging research topics can be tackled at the molecular level.

Materials and methods

Plant Material

Healthy leaves of *Astrocaryum. sciophilum* were collected in August 2017 in the Nouragues national nature reserve, at the Inselberg camp of the CNRS Ecological Research Station, (French Guiana; 4°05’ N - 52°41’W). The identification was carried out by Jerome Chave, scientific director at the EDB (Evolution et Diversité Biologique) laboratory UMR5174, Toulouse. The leaves were sampled by randomly cutting 5x3 cm pieces of fresh leaflets and rachis from individual plants using sterile tweezers. Great care was taken to maintain sterile conditions throughout the process to avoid contamination with the environmental microbiome. The pieces were placed in Eppendorf tubes containing Potato Dextrose Broth ¼ (PDB, Nutriselect™ Basic, Sigma-Aldrich, Germany) medium to allow regrowth of fungi, as

well as tubes containing Cetyl trimethylammonium bromide H6269 (CTAB, CAS: 57-09-0, Sigma-Aldrich, Germany) to preserve genetic material. All the samples were then put in a fridge to slow the growth of fungi during the mission. Around 2 kg of fresh leaves of the same sampled individual *Astrocaryum sciophilum* were collected and dried in an on-site oven for 48h at 40 °C (Fig. 1A). The botanical material was monitored throughout the process and the treatment was stopped when the leaf was sufficiently dry. This procedure was necessary to allow sufficient drying in this type of humid (tropical) environment.

Isolation of endophytes

Isolation of the fungal foliar endophytic community of *A. sciophilum* and establishment of the collection were carried out at the Agroscope in Changins, (Federal Department of Economy, Education and Research, DEFR, Plant Protection Research Division). Each plant fragment stored in PDB tubes was carefully surface sterilized by being washed under a stream of tap water for 3 hours, then subjected to three successive 10-minute baths of sterile water under a laminar flow hood. This surface cleaning without organic solvent was used to reduce possible loss of diversity due to aggressive sterilization using alcoholic solutions. The surface-sterilized leaves were aseptically cut into small segments (0.5 cm^2), placed individually in 9 cm Petri dishes containing potato dextrose agar medium (PDA, Potato Dextrose Agar, Sigma-Aldrich, Germany), amended with aureomycin (25 $ppm.L^{-1}$) (to avoid the growth of bacteria and promote the growth of fungi only) cultured at room temperature, and inspected daily for the emergence of fungi. Each individual emerging hyphal tip was removed and transferred on fresh 9 cm Petri dishes containing PDA and aureomycin. Each individual emerging hyphal fragment was isolated and grown separately. This yielded a collection of 15 strains of cultivable endophytes (Fig. 1B). The isolated and selected strains were then individually cultured on a small scale in 9 cm Petri dishes containing PDA without aureomycin.

Identification of fungal strains

Identification of the isolated strains was performed by extraction of the ribosomal DNA (phenol/choroform), PCR amplification of the ITS1F and ITS4 region and sequencing (Fasteris, Geneva, Switzerland). The obtained sequences were then submitted to BLAST® in GenBank (GB, NCBI https://blast.ncbi.nlm.nih.gov/Blast.cgi) to identify the strain, following Hoftstetter *et al.* (2019) (Hofstetter et al., 2019). The specimens were integrated into the dynamic fungal library of Agroscope, whose content is available on the web (database Mycoscope: https://www.mycoscope.ch/) under the references numbers 1883-91, 1894-96

and 1981 in vials containing 5 ml of diluted PDB aqueous solution (1:4) at 4 °C. The species identified for those strains are listed, per strain number, in Table S1.

Culture and extraction of the isolated foliar fungal endophytes

Small-scale cultures were obtained by central inoculation of a 0.5 cm^3 plug of agar (PDA medium) from the initial pure strain culture into the center of 9 cm Petri dishes containing PDA, repeated on 10 Petri dishes, and cultivated at room temperature until the complete covering of the plate by the mycelium. The culture medium of the 10 cultures of each strain was then collected, cut in small pieces mixed with ethyl acetate (EtOAc, Thommen-Furler, Bern, Switzerland), and extracted by maceration in for 24 h under agitation at room temperature. The organic phase was recovered by vacuum filtration and washed three times with Millipore Corporation (MilliQ) water (Elga Lab-Water, High Wycombe, UK). The organic (Et) and water (W) phases were dried under reduced pressure with a rotary evaporator (Büchi, Flawil, Switzerland) to yield crude mixtures. Agar from uninoculated PDA plates was treated the same way and used as control.

Plant extraction

The oven-dried leaves of *A. sciophilum* were ground to a thin powder. The ground material (760 g) was then successively extracted under maceration and agitation using a sequence of solvents of increasing polarity (hexane, ethyl acetate, methanol (Thommen-Furler AG, Bern, Switzerland) and MilliQ water) and concentrated under reduced pressure to yield 4 extracts: hexane (19.9 g), ethyl acetate (10.7 g), methanol (58.2 g), and water (15.3 g) extract.

Preparative MPLC-UV fractionation of the EtOAc leaf extract

The MPLC column (460x49 mm, 25 µm, i.d., Büchi) was packed with Silicagel 60Å (40-63 µm, Merck) as stationary phase. The plant extract was introduced in MPLC using a dry load cell: 8 g of extract were mixed with 27 g of stationary phase (Silicagel 60Å, 40-63 µm), with a ratio (1:3, extract:stationary phase) in 500 mL of HPLC grade EtOAc (Thermo Fisher Scientific, Waltham, USA), then evaporated to dryness to give 35.13 g of a homogeneous powder in which 1g of sand was added. The powder was then placed into a dry load cell (special aluminum column of 11.5 x 2.7 cm, connecting the pumps and the MPLC column, allowing a higher pressure than with the usual glass precolumn (Challal et al., 2015)) between of two layers of sand. The optimized normal-phase analytical HPLC (NP-HPLC) conditions were geometrically transferred to the preparative MPLC system (Guillarme et al., 2008). Analytical NP-HPLC analyses were conducted as follows: Scorpio Si 60 Å column

(250x4.6 mm, 15 μm spherical, BGB); solvent system hexane (A), EtOAc (B); separation with a gradient step from 10 to 25 % of B over 2 min, isocratic step at 25 % of B over 23 min, gradient step from 25 to 60 % of B over 20 min, and 60 to 100 % of B over 15 min held for 10 min; flow rate fixed at 1mL/min; UV detection recorded at 210, 254, 280, 366 nm. Preparative MPLC conditions were as follows: MPLC column (460x49 mm, 25 μm, i.d.) packed with Silicagel 60 Å (40-63 μm); solvent system hexane (A), EtOAc (B); separation with a gradient step from 10 to 25 % of B over 14 min, isocratic step at 25 % of B over 109 min, gradient step from 25 to 60 % of B over 94 min, and 60 to 100 % of B over 71 min held for 48 min; flow rate fixed at 40 mL/min. UV detection recorded at 254, 280, 366 and 560 nm. The separation yielded 50 fractions of 250 mL that were dried under reduced pressure with a rotary evaporator. The MPLC fractions were then monitored by UHPLC-UV-ELSD-QDa analyses of the MPLC fractions were performed Acquity UHPLC system interfaced to a QDa mass spectrometer (Waters®, Milford, USA) and using electrospray ionization (HESI-II) source. Chromatographic separations were performed as follows: Acquity BEH C18 column (2.1 x 50 mm; 1.7 μm); solvent system water (A), acetonitrile (B), both with 0.1 % FA; separation with a linear gradient from 5 to 100 % of B in 7 min and a 1 min isocratic step at 100 % of B; flow rate fixed at 600 μL/min; temperatures autosampler and column oven at 10 and 40 °C. UV data acquired from 200 to 600 nm; ELSD temperature at 45 °C; pressure at 3.5 bar; gain at 8. Mass data were obtained by a fully automated acquisition at 10 Hz for *m/z* between 100 and 1000. Data acquisition, instrument control and data processing were performed with the Masslynx® software (Waters®).

Mass spectrometry analysis

UHPLC-HRMS/MS metabolite profiling

Chromatographic separation was achieved on a Waters Acquity UPLC system interfaced to a Q-exactive Focus mass spectrometer (Thermo Scientific, Bremen, Germany) using a heated electrospray ionsization (HESI-II) source. Thermo Scientific Xcalibur 3.1 software was used for instrument control. LC separation was conducted as follow: Acquity BEH C18 column (2.1 x 50 mm; 1.7 m, Waters); mobile phase, water (A), acetonitrile (B) both with 0.1 % formic acid;

flow rate fixed at 600 μL/min; injection volume 4 μL; linear gradient from 5 to 100 % of B in 7 min and isocratic at 100 % of B for 1 min. The optimized HESI-II parameters were as follows: source voltage, 3.5 kV (pos), 4 kV (neg); sheath gas flow rate (N_2), 55 units;

auxiliary gas flow rate, 15 units; spare gas flow rate, 3.0; capillary temperature, 275 °C (pos), 320 °C (neg); S-Lens RF Level, 45. The mass analyzer was calibrated using a mixture of caffeine, methionine-arginine-alanine-acetate (MRFA), sodium dodecyl sulfate, sodium taurocholate and Ultramark 1621 in an acetonitrile/methanol/water solution containing 1 % formic acid by direct injection.

The data-dependent MS/MS events were performed on the three most intense ions detected in full scan MS (Top3 experiment). The MS/MS isolation window width was 1 Da, and the normalized collision energy was set to 15, 30, and 45 units. In data dependent MS/MS experiments, full scans were acquired at a resolution of 35,000 FWHM (at *m/z* 200) and MS/MS scans at 17,500 FWHM both with an automatically determined maximum injection time. After being acquired in a MS/MS scan, precursors ions were placed in a dynamic exclusion list for 2.0 s. Detection was performed in positive ion mode (PI) and in negative ion mode (NI) with an *m/z* scan range of 130–1950.

Leaf MPLC fractions and EtOAc crude extract (48 samples) were analyzed in the first part of the series, fungal extracts (34 samples) in the second part of the series, with a thorough cleaning step with blank samples to ensure no interference between the 2 series. Samples were analyzed in analytical triplicates and in random order (48×3+30×3=234 samples). Quality controls (QC, equal mixture of all the samples for each series), and blank samples (injection solvent only) were included every 10 runs. Blank PDA samples (extracted uninoculated culture media) were also added. In addition, 5 analyses of both blank and QC samples were included before and after the analyses of both sets. Analytical standards and molecules isolated from some of the strains individually investigated in our laboratory were also analyzed in a separate set.

UHPLC-HRMS/MS data processing

The UHPLC-HRMS/MS data were converted from .RAW (Thermo) standard data format into .mzXML format using the MS convert software (ProteoWizard package (Chambers et al., 2012)). The converted files were processed using MZmine (v2.51) (Pluskal et al., 2010), all the previously described samples were processed in the same batch of MZmine analyses, to allow for comparison of MS data. Mass detection was carried out using a centroid mass detector with a noise level set at 4E5 (1E4 NI) for MS level 1, and at 0 for MS level 2. The ADAP chromatogram builder was employed and set to a minimum group size of scans of 5, a minimum group intensity threshold of 4E5 (1E4 NI), a minimum highest intensity of 4E5

(1E4 NI) and a *m/z* tolerance of 8.0 ppm. The wavelets ADAP algorithm was used for chromatogram deconvolution with the following settings: intensity window single to noise (S/N) as S/N estimator with S/N threshold set at 15 (20 NI), a minimum feature height at 4E5 (1E4 NI), coefficient area threshold at 150 (100 NI), peak duration range 0.02 to 0.9 min (0.02-0.8 NI), wavelet range 0.01 to 0.04 min. Isotopes were detected using the isotope peak grouper with *m/z* tolerance set at 8.0 ppm, RT tolerance at 0.02 min (absolute), maximum charge of 2, representative isotope as the most intense. Each feature list was filtered before alignment to remove duplicates using the duplicate peak filter with RT tolerance at 0.03 min and *m/z* tolerance at 8 ppm, and to keep only features with an associated MS2 scan using the peak list row filter. Peak alignment was performed using the join aligner method with *m/z* tolerance at 10 ppm, absolute RT tolerance at 0.04 min, weight for *m/z* and RT at 10, and a weighted dot-product cosine similarity at 0.7. A local spectra database (DB) search identification was finally conducted using a custom DB (.msp file) containing MS data of standards and previously isolated molecules ran in the same batch of analyses, with *m/z* tolerance at 20 ppm and weighted dot-product cosine similarity at 0.8. The aligned feature list was exported using the GNPS export module.

Feature table processing

A unique feature table of the 246 samples, and blanks was obtained. The table was filtered by subtracting peaks from the blank and the media and by only keeping the features detected in the 3 replicates of at least one sample. To establish the co-occurrence of a given retained feature in the other samples, its detection had to be recorded at least in 2 replicates. The intensities were then normalized by feature (sum of the intensities in the different samples for each ion = 1). The average intensity of the three replicates was then calculated for each feature considered. This overall filtering process led to the discard of around 33205 features out of 57301 from the initial table for positive ionization (PI) analyses and 8775 out of 19567 for negative ionization (NI) analyses. This led to a final feature list: **general dataset** = 24096 features (PI), 10792 (NI). This feature list was then filtered based on the sample origin from all fungal samples on one side and all leaf samples on the other, to yield 2 feature lists: **fungal dataset** = 11072 (PI), 5982 (NI), **host dataset** = 13884 (PI), 5503 (NI). The .mgf files associated with each data set were then extracted to allow the molecular network processing. The mass spectrometry data were deposited on the MassIVE public repository n° MSV000088516.

Molecular Networks (MN) generation

In order to maintain the RT and exact mass information and to allow for isomer separation, feature based MN were created using the .mgf file resulting from the MZmine pretreatment steps detailed above (FBMN). Spectral data were then uploaded on the GNPS MN platform. A MN was created where edges were filtered to have a cosine score above 0.7 and more than 6 matched peaks. Further, edges between two nodes were kept in the network if, and only if, each of the nodes appeared in each other's respective top 10 most similar nodes. Finally, the maximum size of a molecular family was set to 100, and the lowest scoring edges were removed from molecular families until the molecular family size was below this threshold. The spectra in the network were then searched against GNPS spectral libraries (Wang et al., 2016). All matches kept between network spectra and library spectra were required to have a score above 0.7 and at least 6 matched peaks. The output was visualized using Cytoscape software v3.8.0 (Shannon et al., 2003). The different GNPS jobs parameters and resulting data are available at the following addresses:

PI fungal dataset:
https://gnps.ucsd.edu/ProteoSAFe/status.jsp?task=28f944e757d54755948824ca55e4a601
PI host dataset:
https://gnps.ucsd.edu/ProteoSAFe/status.jsp?task=75c277bd53a341ff826f63ea4d1a0e3e
PI general dataset:
https://gnps.ucsd.edu/ProteoSAFe/status.jsp?task=250536f4cb3e4f159e5ef67a3d024fac
NI fungal dataset:
https://gnps.ucsd.edu/ProteoSAFe/status.jsp?task=b28bfcec6019409ca75c6aae0348eccf
NI host dataset:
https://gnps.ucsd.edu/ProteoSAFe/status.jsp?task=d87595a93200444286531b89e1ffb692
NI general dataset:
https://gnps.ucsd.edu/ProteoSAFe/status.jsp?task=b786792e271d46bbb6816853f69eeb25

Class annotation for the whole dataset

Filtered features detected in PI in the general dataset were annotated using a computational approach integrating SIRIUS (molecular formula), CSI:fingerID (probabilistic molecular fingerprint by machine learning substructure prediction and *in silico* annotation) and CANOPUS (systematic class annotation) (Dührkop et al., 2015, 2019, 2021). SIRIUS analyzes both isotope and fragmentation patterns to determine the molecular formula of the measured precursor ions. Furthermore, it uses CSI:fingerID to predict a molecular fingerprint from the related MS/MS spectrum and fragmentation tree and to propose putative annotations by searching in a molecular structure databases. Finally, CANOPUS predicts compound chemical classes, using NPClassifier taxonomy, from the molecular fingerprint generated by CSI:FingerID (Dührkop et al., 2015, 2019, 2021).

Taxonomically informed metabolite annotation

The spectral files (.mgf) and attributes metadata (.clustersummary) obtained after the MN step were annotated firstly at the MS1 level by matching the precursor *m/z* with all the potential *m/z* of the most common adducts of the compounds reported in the taxonomic family of the analyzed sample, secondly at the MS/MS level against a custom version of the LOTUS-ISDB (in-house database containing the *in silico* fragmentation spectra of all the compounds present in the DNP and LOTUS databases) complemented with structure-organism pairs coming from the Dictionary of Natural Products DNP (Zenodo) (Allard et al., 2016; Rutz et al., 2019). The following parameters were used: spectral match parameters: parent mass tolerance 0.01 Da, MS/MS tolerance 0.01 Da, minimum cosine score 0.2, minimum peaks 6. Spectral match of MS/MS spectra against the database provided a list of 50 chemical structure candidates for every feature. The candidates were re-ranked by taxonomic reweighting after ponderation of their spectral score inversely proportional to the taxonomic distance between the biological source of the candidate and that of the one of analyzed sample(s) (e.g the fungal strain) in which the feature is detected (Rutz et al., 2019). Based on the MN topology, a consensus chemical class at each NPclassifier level (Kim et al., 2021) (pathway, superclass, class) was returned for every node, and annotations were re-ranked accordingly. The top 3 candidates were finally retained.

Interactive plot GitHub repository: leonie74/leonie74.github.io

Acknowledgments

The authors acknowledge the Agence Nationale de la Recherche and the Swiss National Science Foundation for the funding of the SECIL project (SECIL, ref ANR-15-CE21-0016 and SNF n°310030E-164289). The authors thank Oliver PAUL for its contribution to the creation of the online visualizations of interactive plots (leonie74/leonie74.github.io).

References

Agostini-Costa, T. da S. (2018). Bioactive compounds and health benefits of some palm species traditionally used in Africa and the Americas – A review. *J. Ethnopharmacol.* 224, 202–229. doi: 10.1016/j.jep.2018.05.035.

Allard, P.-M., Péresse, T., Bisson, J., Gindro, K., Marcourt, L., Pham, V. C., et al. (2016). Integration of molecular networking and in-silico MS/MS fragmentation for natural products dereplication. *Anal. Chem.* 88, 3317–3323. doi: 10.1021/acs.analchem.5b04804.

Amaral, L. da S., Rodrigues-Filho, E., Santos, C. A. A., de Abreu, L. M., and Pfenning, L. H. (2014). An HPLC evaluation of cytochalasin D biosynthesis by *Xylaria arbuscula* cultivated in different media. *Nat. Prod. Commun.* 9, 1934578X1400900914. doi: 10.1177/1934578X1400900914.

Arnold, A. E. (2007). Understanding the diversity of foliar endophytic fungi: progress, challenges, and frontiers. *Fungal Biol. Rev.* 21, 51–66. doi: 10.1016/j.fbr.2007.05.003.

Arnold, A. E., Mejía, L. C., Kyllo, D., Rojas, E. I., Maynard, Z., Robbins, N., et al. (2003). Fungal endophytes limit pathogen damage in a tropical tree. *Proc. Natl. Acad. Sci.* 100, 15649–15654. doi: 10.1073/pnas.2533483100.

Athenaki, M., Gardeli, C., Diamantopoulou, P., Tchakouteu, S. s., Sarris, D., Philippoussis, A., et al. (2018). Lipids from yeasts and fungi: physiology, production and analytical considerations. *J. Appl. Microbiol.* 124, 336–367. doi: 10.1111/jam.13633.

Barthélémy, M. (2019). Etude de la diversité chimique et biologique d'endophytes de palmiers. Available at: https://tel.archives-ouvertes.fr/tel-03173515 [Accessed November 29, 2021].

Bonneville, S., Delpomdor, F., Préat, A., Chevalier, C., Araki, T., Kazemian, M., et al. (2020). Molecular identification of fungi microfossils in a Neoproterozoic shale rock. *Sci. Adv.* 6. doi: 10.1126/sciadv.aax7599.

Böttcher, C., and Pollmann, S. (2009). Plant oxylipins: Plant responses to 12-oxo-phytodienoic acid are governed by its specific structural and functional properties. *FEBS J.* 276, 4693–4704. doi: 10.1111/j.1742-4658.2009.07195.x.

Brader, G., Compant, S., Mitter, B., Trognitz, F., and Sessitsch, A. (2014). Metabolic potential of endophytic bacteria. *Curr. Opin. Biotechnol.* 27, 30–37. doi: 10.1016/j.copbio.2013.09.012.

Brodhun, F., and Feussner, I. (2011). Oxylipins in fungi. *FEBS J.* 278, 1047–1063. doi: 10.1111/j.1742-4658.2011.08027.x.

Calvo, A. M., Hinze, L. L., Gardner, H. W., and Keller, N. P. (1999). Sporogenic effect of polyunsaturated fatty acids on development of *Aspergillus* spp. *Appl. Environ. Microbiol.* 65, 3668–3673. doi: 10.1128/AEM.65.8.3668-3673.1999.

Capasso, R., Evidente, A., and Vurro, M. (1991). Cytochalasins from *Phoma exigua* var. *heteromorpha*. *Phytochemistry* 30, 3945–3950. doi: 10.1016/0031-9422(91)83442-N.

Castro-Moretti, F. R., Gentzel, I. N., Mackey, D., and Alonso, A. P. (2020). Metabolomics as an emerging tool for the study of plant–pathogen interactions. *Metabolites* 10, 52. doi: 10.3390/metabo10020052.

Challal, S., Queiroz, E. F., Debrus, B., Kloeti, W., Guillarme, D., Gupta, M. P., et al. (2015). Rational and efficient preparative isolation of natural products by MPLC-UV-ELSD based on HPLC to MPLC gradient transfer. *Planta Med.* 81, 1636–1643. doi: 10.1055/s-0035-1545912.

Chambers, M. C., Maclean, B., Burke, R., Amodei, D., Ruderman, D. L., Neumann, S., et al. (2012). A cross-platform toolkit for mass spectrometry and proteomics. *Nat. Biotechnol.* 30, 918–920. doi: 10.1038/nbt.2377.

Charles-Dominique, P., Chave, J., Dubois, M.-A., De Granville, J.-J., Riera, B., and Vezzoli, C. (2003). Colonization front of the understorey palm *Astrocaryum sciophilum* in a pristine rain forest of French Guiana. *Glob. Ecol. Biogeogr.* 12, 237–248.

Chen, Z., Chen, H.-P., Li, Y., Feng, T., and Liu, J.-K. (2015). Cytochalasins from cultures of endophytic fungus *Phoma multirostrata* EA-12. *J. Antibiot. (Tokyo)* 68, 23–26. doi: 10.1038/ja.2014.87.

Chen, Z., Chen, Y., Huang, H., Yang, H., Zhang, W., Sun, Y., et al. (2017). Cytochalasin P1, a new cytochalasin from the marine-derived fungus *Xylaria* sp. SOF11. *Z. Für Naturforschung C* 72, 129–132. doi: 10.1515/znc-2016-0122.

Christensen, S. A., and Kolomiets, M. V. (2011). The lipid language of plant–fungal interactions. *Fungal Genet. Biol.* 48, 4–14. doi: 10.1016/j.fgb.2010.05.005.

Christian, N., Sedio, B. E., Florez- Buitrago, X., Ramírez- Camejo, L. A., Rojas, E. I., Mejía, L. C., et al. (2020). Host affinity of endophytic fungi and the potential for reciprocal interactions involving host secondary chemistry. *Am. J. Bot.* 107, 219–228. doi: 10.1002/ajb2.1436.

Cox, R. H., Morris, P., Cutler, H. G., Hurd, R. E., and Cole, R. J. (1983). Proton and carbon-13 nuclear magnetic resonance studies of the conformation of cytochalasin H derivatives and plant growth regulating effects of cytochalasins. *J. Agric. Food Chem.* 31, 405–408. doi: 10.1021/jf00116a055.

Cox, R. J., Skellam, E., and Williams, K. (2018). "Biosynthesis of Fungal Polyketides," in *Physiology and Genetics: Selected Basic and Applied Aspects* The Mycota., eds. T. Anke and A. Schüffler (Cham: Springer International Publishing), 385–412. doi: 10.1007/978-3-319-71740-1_13.

Darnet, S., Blary, A., Chevalier, Q., and Schaller, H. (2021). Phytosterol Profiles, Genomes and Enzymes – An Overview. *Front. Plant Sci.* 12, 878. doi: 10.3389/fpls.2021.665206.

Dastogeer, K. M. G., Tumpa, F. H., Sultana, A., Akter, M. A., and Chakraborty, A. (2020). Plant microbiome–an account of the factors that shape community composition and diversity. *Curr. Plant Biol.* 23, 100161. doi: 10.1016/j.cpb.2020.100161.

de Oliveira, A. I. T., Mahmoud, T. S., do Nascimento, G. N. L., da Silva, J. F. M., Pimenta, R. S., and de Morais, P. B. (2016). Chemical composition and antimicrobial potential of palm leaf extracts from Babaçu (*Attalea speciosa*), Buriti (*Mauritia flexuosa*), and Macaúba (*Acrocomia aculeata*). *Sci. World J.* 2016, 9734181. doi: 10.1155/2016/9734181.

de Oliveira, D. M., Siqueira, E. P., Nunes, Y. R. F., and Cota, B. B. (2013). Flavonoids from leaves of *Mauritia flexuosa*. *Rev. Bras. Farmacogn.* 23, 614–620. doi: 10.1590/S0102-695X2013005000061.

Devi, P., Shridhar, M. P. D., D'Souza, L., Naik, C. G., and Paula, D. (2006). Cellular fatty acid composition of marine-derived fungi. *Indian J Mar Sci* 35, 5.

Djonović, S., Vargas, W. A., Kolomiets, M. V., Horndeski, M., Wiest, A., and Kenerley, C. M. (2007). A proteinaceous elicitor Sm1 from the beneficial fungus *Trichoderma virens* is required for induced systemic resistance in aize. *Plant Physiol.* 145, 875–889. doi: 10.1104/pp.107.103689.

Donald, J., Barthélemy, M., Gazal, N., Eveno, Y., Manzi, S., Eparvier, V., et al. (2019). Tropical palm endophytes exhibit low competitive structuring when assessed using co-occurrence and antipathogen activity analysis. *Front. For. Glob. Change* 2. doi: 10.3389/ffgc.2019.00086.

Donald, J., Roy, M., Suescun, U., Iribar, A., Manzi, S., Péllissier, L., et al. (2020). A test of community assembly rules using foliar endophytes from a tropical forest canopy. *J. Ecol.* 108, 1605–1616. doi: 10.1111/1365-2745.13344.

Dong, M., Oda, Y., and Hirota, M. (2000). (10 *E* ,12 *Z* ,15 *Z*)-9-Hydroxy-10,12,15-octadecatrienoic acid methyl ester as an anti-inflammatory compound from *Ehretia dicksonii*. *Biosci. Biotechnol. Biochem.* 64, 882–886. doi: 10.1271/bbb.64.882.

Draper, J., Rasmussen, S., and Zubair, H. (2011). "Metabolite analysis and metabolomics in the study of biotrophic interactions between plants and microbes," in *Annual Plant Reviews Volume 43*, ed. R. D. Hall (Oxford, UK: Wiley-Blackwell), 25–59. doi: 10.1002/9781444339956.ch2.

Dührkop, K., Fleischauer, M., Ludwig, M., Aksenov, A. A., Melnik, A. V., Meusel, M., et al. (2019). SIRIUS 4: a rapid tool for turning tandem mass spectra into metabolite structure information. *Nat. Methods* 16, 299–302. doi: 10.1038/s41592-019-0344-8.

Dührkop, K., Nothias, L.-F., Fleischauer, M., Reher, R., Ludwig, M., Hoffmann, M. A., et al. (2021). Systematic classification of unknown metabolites using high-resolution fragmentation mass spectra. *Nat. Biotechnol.* 39, 462–471. doi: 10.1038/s41587-020-0740-8.

Dührkop, K., Shen, H., Meusel, M., Rousu, J., and Böcker, S. (2015). Searching molecular structure databases with tandem mass spectra using CSI:FingerID. *Proc. Natl. Acad. Sci.* 112, 12580–12585. doi: 10.1073/pnas.1509788112.

El-Dib, R., Kaloga, M., Mahmoud, I., Soliman, H. S. M., Moharram, F. A., and Kolodziej, H. (2004). Sablacaurin A and B, two 19-nor-3,4-seco-lanostane-type triterpenoids from *Sabal causiarum* and *Sabal blackburniana*, respectively. *Phytochemistry* 65, 1153–1157. doi: 10.1016/j.phytochem.2004.02.026.

Epp, L. S., Boessenkool, S., Bellemain, E. P., Haile, J., Esposito, A., Riaz, T., et al. (2012). New environmental metabarcodes for analysing soil DNA: potential for studying past and present ecosystems. *Mol. Ecol.* 21, 1821–1833. doi: 10.1111/j.1365-294X.2012.05537.x.

Estrada, C., Wcislo, W. T., and Bael, S. A. V. (2013). Symbiotic fungi alter plant chemistry that discourages leaf-cutting ants. *New Phytol.* 198, 241–251. doi: 10.1111/nph.12140.

Feitosa, A. de O., Dias, A. C. S., Ramos, G. da C., Bitencourt, H. R., Siqueira, J. E. S., Marinho, P. S. B., et al. (2016). Lethality of cytochalasin B and other compounds isolated from fungus *Aspergillus* sp. (Trichocomaceae) endophyte of *Bauhinia guianensis* (Fabaceae). *Rev. Argent. Microbiol.* 48, 259–263. doi: 10.1016/j.ram.2016.04.002.

Fernandes, C. M., Goldman, G. H., and Del Poeta, M. (2018). Biological roles played by sphingolipids in dimorphic and filamentous fungi. *mBio* 9. doi: 10.1128/mBio.00642-18.

Fiorilli, V., Wang, J. Y., Bonfante, P., Lanfranco, L., and Al-Babili, S. (2019). Apocarotenoids: old and new mediators of the arbuscular mycorrhizal symbiosis. *Front. Plant Sci.* 10, 1186. doi: 10.3389/fpls.2019.01186.

Gao, X., and Kolomiets, M. V. (2009). Host-derived lipids and oxylipins are crucial signals in modulating mycotoxin production by fungi. *Toxin Rev.* 28, 79–88. doi: 10.1080/15569540802420584.

Glenn, A. E., Hinton, D. M., Yates, I. E., and Bacon, C. W. (2001). Detoxification of corn antimicrobial compounds as the basis for isolating *Fusarium verticillioides* and some other *Fusarium* Species from corn. *Appl. Environ. Microbiol.* 67, 2973–2981. doi: 10.1128/AEM.67.7.2973-2981.2001.

Griffin, D. H. (1996). *Fungal Physiology*. John Wiley & Sons.

Guillarme, D., Nguyen, D. T. T., Rudaz, S., and Veuthey, J.-L. (2008). Method transfer for fast liquid chromatography in pharmaceutical analysis: application to short columns packed with small particle. Part II: gradient experiments. *Eur. J. Pharm. Biopharm. Off. J. Arbeitsgemeinschaft Pharm. Verfahrenstechnik EV* 68, 430–440. doi: 10.1016/j.ejpb.2007.06.018.

Hansson, D., Wubshet, S., Olson, Å., Karlsson, M., Staerk, D., and Broberg, A. (2014). Secondary metabolite comparison of the species within the *Heterobasidion annosum* s.l. complex. *Phytochemistry* 108, 243–251. doi: 10.1016/j.phytochem.2014.08.028.

He, M., Qin, C.-X., Wang, X., and Ding, N.-Z. (2020). Plant unsaturated fatty acids: biosynthesis and regulation. *Front. Plant Sci.* 11, 390. doi: 10.3389/fpls.2020.00390.

Hofstetter, V., Buyck, B., Eyssartier, G., Schnee, S., and Gindro, K. (2019). The unbearable lightness of sequenced-based identification. *Fungal Divers.* 96, 243–284. doi: 10.1007/s13225-019-00428-3.

Howitz, K. T., and Sinclair, D. A. (2008). Xenohormesis: sensing the chemical cues of other species. *Cell* 133, 387–391. doi: 10.1016/j.cell.2008.04.019.

Jung, H. W., Tschaplinski, T. J., Wang, L., Glazebrook, J., and Greenberg, J. T. (2009). Priming in systemic plant immunity. *Science* 324, 89–91. doi: 10.1126/science.1170025.

Kahn, F. (2008). The genus *Astrocaryum* (Arecaceae). *Rev. Peru. Biol.* 15, 29–46.

Khatri, Y., Girhard, M., Romankiewicz, A., Ringle, M., Hannemann, F., Urlacher, V. B., et al. (2010). Regioselective hydroxylation of norisoprenoids by CYP109D1 from *Sorangium cellulosum* So ce56. *Appl. Microbiol. Biotechnol.* 88, 485–495. doi: 10.1007/s00253-010-2756-3.

Khiralla, A., Spina, R., Saliba, S., and Laurain-Mattar, D. (2019). Diversity of natural products of the genera *Curvularia* and *Bipolaris*. *Fungal Biol. Rev.* 33, 101–122. doi: 10.1016/j.fbr.2018.09.002.

Kim, H., Wang, M., Leber, C., Nothias, L.-F., Reher, R., Kang, K. B., et al. (2021). NPClassifier: A deep neural network-based structural classification tool for natural products. *J. Nat. Prod.* 84, 2795–2807. doi: 10.1021/acs.jnatprod.1c00399.

Klemptner, R. L., Sherwood, J. S., Tugizimana, F., Dubery, I. A., and Piater, L. A. (2014). Ergosterol, an orphan fungal microbe-associated molecular pattern (MAMP). *Mol. Plant Pathol.* 15, 747–761. doi: 10.1111/mpp.12127.

Kobayashi, Y., Yamada, M., Kobayashi, I., and Kunoh, H. (1997). Actin microfilaments are required for the expression of nonhost resistance in higher plants. *Plant Cell Physiol.* 38, 725–733. doi: https://doi.org/10.1093/oxfordjournals.pcp.a029226.

Kusari, S., Pandey, S. P., and Spiteller, M. (2013). Untapped mutualistic paradigms linking host plant and endophytic fungal production of similar bioactive secondary metabolites. *Phytochemistry* 91, 81–87. doi: 10.1016/j.phytochem.2012.07.021.

Kusumah, D., Wakui, M., Murakami, M., Xie, X., Yukihito, K., and Maeda, I. (2020). Linoleic acid, α-linolenic acid, and monolinolenins as antibacterial substances in the heat-processed soybean fermented with *Rhizopus oligosporus*. *Biosci. Biotechnol. Biochem.* 84, 1285–1290. doi: 10.1080/09168451.2020.1731299.

Lastovetsky, O. A., Gaspar, M. L., Mondo, S. J., LaButti, K. M., Sandor, L., Grigoriev, I. V., et al. (2016). Lipid metabolic changes in an early divergent fungus govern the establishment of a mutualistic symbiosis with endobacteria. *Proc. Natl. Acad. Sci.* 113, 15102–15107. doi: 10.1073/pnas.1615148113.

Leach, J. E., Triplett, L. R., Argueso, C. T., and Trivedi, P. (2017). Communication in the Phytobiome. *Cell* 169, 587–596. doi: 10.1016/j.cell.2017.04.025.

Lucaciu, R., Pelikan, C., Gerner, S. M., Zioutis, C., Köstlbacher, S., Marx, H., et al. (2019). A Bioinformatics guide to plant microbiome analysis. *Front. Plant Sci.* 10. doi: 10.3389/fpls.2019.01313.

Ludwig-Müller, J. (2015). Plants and endophytes: equal partners in secondary metabolite production? *Biotechnol. Lett.* 37, 1325–1334. doi: 10.1007/s10529-015-1814-4.

Luo, X., Yang, J., Chen, F., Lin, X., Chen, C., Zhou, X., et al. (2018). Structurally diverse polyketides from the mangrove-derived fungus *Diaporthe* sp. SCSIO 41011 with their anti-influenza A virus activities. *Front. Chem.* 6, 282. doi: 10.3389/fchem.2018.00282.

Ma, J.-T., Du, J.-X., Zhang, Y., Liu, J.-K., Feng, T., and He, J. (2022). Natural imidazole alkaloids as antibacterial agents against *Pseudomonas syringae* pv. *actinidiae* isolated from kiwi endophytic fungus *Fusarium tricinctum*. *Fitoterapia* 156, 105070. doi: 10.1016/j.fitote.2021.105070.

Macabuhay, A., Arsova, B., Walker, R., Johnson, A., Watt, M., and Roessner, U. (2021). Modulators or facilitators? Roles of lipids in plant root–microbe interactions. *Trends Plant Sci.* doi: 10.1016/j.tplants.2021.08.004.

Martin, F. M., Uroz, S., and Barker, D. G. (2017). Ancestral alliances: Plant mutualistic symbioses with fungi and bacteria. *Science* 356, eaad4501. doi: 10.1126/science.aad4501.

Mattoo, A. J., and Nonzom, S. (2021). Endophytic fungi: understanding complex cross-talks. *Symbiosis* 83, 237–264. doi: 10.1007/s13199-020-00744-2.

Mejía, L. C., Herre, E. A., Sparks, J. P., Winter, K., García, M. N., Van Bael, S. A., et al. (2014). Pervasive effects of a dominant foliar endophytic fungus on host genetic and phenotypic expression in a tropical tree. *Front. Microbiol.* 5. doi: 10.3389/fmicb.2014.00479.

Miersch, O., Bohlmann, H., and Wasternack, C. (1999). Jasmonates and related compounds from *Fusarium oxysporum*. *Phytochemistry* 50, 517–523. doi: 10.1016/S0031-9422(98)00596-2.

Mingrone, G., and Castagneto, M. (2006). Medium-chain, even-numbered dicarboxylic acids as novel energy substrates: an update. *Nutr. Rev.* 64, 449–456. doi: 10.1301/nr.2006.oct.449-456.

Mishra, A. K., Choi, J., Choi, S.-J., and Baek, K.-H. (2017). Cyclodipeptides: An Overview of Their Biosynthesis and Biological Activity. *Molecules* 22, 1796. doi: 10.3390/molecules22101796.

Moffatt, B. A., and Ashihara, H. (2002). Purine and pyrimidine nucleotide synthesis and metabolism. *Arab. Book* 2002. doi: 10.1199/tab.0018.

Nes, W. D., Xu, S. H., and Haddon, W. F. (1989). Evidence for similarities and differences in the biosynthesis of fungal sterols. *Steroids* 53, 533–558. doi: 10.1016/0039-128x(89)90030-5.

Nisar, N., Li, L., Lu, S., Khin, N. C., and Pogson, B. J. (2015). Carotenoid metabolism in plants. *Mol. Plant* 8, 68–82. doi: 10.1016/j.molp.2014.12.007.

Noronha Matos, K. A., Praia Lima, D., Pereira Barbosa, A. P., Zerlotti Mercadante, A., and Campos Chisté, R. (2019). Peels of tucumã (*Astrocaryum vulgare*) and peach palm (*Bactris gasipaes*) are by-products classified as very high carotenoid sources. *Food Chem.* 272, 216–221. doi: 10.1016/j.foodchem.2018.08.053.

Noverr, M. C., Erb-Downward, J. R., and Huffnagle, G. B. (2003). Production of ecosanoids and other oxylipins by pathogenic eukaryotic microbes. *Clin. Microbiol. Rev.* 16, 517–533. doi: 10.1128/CMR.16.3.517-533.2003.

Pang, G., Sun, T., Yu, Z., Yuan, T., Liu, W., Zhu, H., et al. (2020). Azaphilones biosynthesis complements the defence mechanism of *Trichoderma guizhouense* against oxidative stress. *Environ. Microbiol.* 22, 4808–4824. doi: 10.1111/1462-2920.15246.

Pluskal, T., Castillo, S., Villar-Briones, A., and Orešič, M. (2010). MZmine 2: Modular framework for processing, visualizing, and analyzing mass spectrometry-based molecular profile data. *BMC Bioinformatics* 11. doi: 10.1186/1471-2105-11-395.

Qiu, X., Xie, X., and Meesapyodsuk, D. (2020). Molecular mechanisms for biosynthesis and assembly of nutritionally important very long chain polyunsaturated fatty acids in microorganisms. *Prog. Lipid Res.* 79, 101047. doi: 10.1016/j.plipres.2020.101047.

Rodrigues, M. L. (2018). The multifunctional fungal ergosterol. *mBio* 9. doi: 10.1128/mBio.01755-18.

Rodríguez-Bustamante, E., Maldonado-Robledo, G., Ortiz, M. A., Díaz-Ávalos, C., and Sanchez, S. (2005). Bioconversion of lutein using a microbial mixture—maximizing the production of tobacco aroma compounds by manipulation of culture medium. *Appl. Microbiol. Biotechnol.* 68, 174–182. doi: 10.1007/s00253-004-1868-z.

Rosenberg, E., and Zilber-Rosenberg, I. (2016). Microbes drive evolution of animals and plants: the hologenome concept. *mBio*. doi: 10.1128/mBio.01395-15.

Roy, S., and Banerjee, D. (2018). "Diversity of endophytes in tropical forests," in *Endophytes of Forest Trees: Biology and Applications* Forestry Sciences., eds. A. M. Pirttilä and A. C. Frank (Cham: Springer International Publishing), 43–62. doi: 10.1007/978-3-319-89833-9_3.

Rutz, A., Dounoue-Kubo, M., Ollivier, S., Bisson, J., Bagheri, M., Saesong, T., et al. (2019). Taxonomically informed scoring enhances confidence in natural products annotation. *Front. Plant Sci.* 10. doi: 10.3389/fpls.2019.01329.

Sadat, M. A., Jeon, J., Mir, A. A., Choi, J., Choi, J., and Lee, Y.-H. (2014). Regulation of cellular diacylglycerol through lipid phosphate phosphatases Is required for pathogenesis of the rice blast fungus, *Magnaporthe oryzae*. *PLOS ONE* 9, e100726. doi: 10.1371/journal.pone.0100726.

Salvatore, M. M., Alves, A., and Andolfi, A. (2020). Secondary metabolites of *Lasiodiplodia theobromae*: distribution, chemical diversity, bioactivity, and implications of their occurrence. *Toxins* 12, 457. doi: 10.3390/toxins12070457.

Sánchez-Contreras, A., Jiménez, M., and Sanchez, S. (2000). Bioconversion of lutein to products with aroma. *Appl. Microbiol. Biotechnol.* 54, 528–534. doi: 10.1007/s002530000421.

Sbrebryakov, E. P., Simolin, A. V., Kucherov, V. F., and Rosynov, B. V. (1970). New metabolites of *Fusarium moniliforme* sheld. *Tetrahedron* 26, 5215–5223. doi: 10.1016/S0040-4020(01)98730-7.

Schaller, F. (2001). Enzymes of the biosynthesis of octadecanoid- derived signalling molecules. *J. Exp. Bot.* 52, 11–23. doi: 10.1093/jexbot/52.354.11.

Schulz, B., and Boyle, C. (2005). The endophytic continuum. *Mycol. Res.* 109, 661–686. doi: 10.1017/S095375620500273X.

Shahnazi, S., Meon, S., and Ebrahimi, M. (2013). Characterisation, differentiation and biochemical diversity of *Fusarium solani* and *Fusarium proliferatum* based on cellular fatty acid profiles. *Arch. Für Phytopathol. Pflanzenschutz*. doi: 10.1080/03235408.2013.770653.

Shannon, P., Markiel, A., Ozier, O., Baliga, N. S., Wang, J. T., Ramage, D., et al. (2003). Cytoscape: a software environment for integrated models of biomolecular interaction networks. *Genome Res.* 13, 2498–2504. doi: 10.1101/gr.1239303.

Siebers, M., Brands, M., Wewer, V., Duan, Y., Hölzl, G., and Dörmann, P. (2016). Lipids in plant–microbe interactions. *Biochim. Biophys. Acta BBA - Mol. Cell Biol. Lipids* 1861, 1379–1395. doi: 10.1016/j.bbalip.2016.02.021.

Sims, J. W., Fillmore, J. P., Warner, D. D., and Schmidt, E. W. (2005). Equisetin biosynthesis in *Fusarium heterosporum*. *Chem. Commun.*, 186–188. doi: 10.1039/B413523G.

Stierle, A., Strobel, G., and Stierle, D. (1993). Taxol and taxane production by *Taxomyces andreanae*, an endophytic fungus of Pacific yew. *Science* 260, 214–216. doi: 10.1126/science.8097061.

Subudhi, E., Sahoo, R. K., Dey, S., Das, A., and Sahoo, K. (2019). "Unraveling plant-endophyte interactions: an omics insight," in *Endophytes and Secondary Metabolites* Reference Series in Phytochemistry., ed. S. Jha (Cham: Springer International Publishing), 249–267. doi: 10.1007/978-3-319-90484-9_2.

Tan, R. X., and Zou, W. X. (2001). Endophytes: a rich source of functional metabolites. *Nat. Prod. Rep.* 18, 448–459. doi: 10.1039/ b100918o.

Tapondjou, L. A., Siems, K. J., Böttger, S., and Melzig, M. F. (2015). Steroidal saponins from the mesocarp of the fruits of *Raphia farinifera* (Arecaceae) and their cytotoxic activity. *Nat. Prod. Commun.* 10, 1934578X1501001134. doi: 10.1177/1934578X1501001134.

Tiwari, P., and Bae, H. (2020). Horizontal gene transfer and endophytes: an implication for the acquisition of novel traits. *Plants* 9, 305. doi: 10.3390/plants9030305.

Toljamo, A., Koistinen, V., Hanhineva, K., Kärenlampi, S., and Kokko, H. (2021). Terpenoid and lipid profiles vary in different *Phytophthora cactorum* – strawberry interactions. *Phytochemistry* 189, 112820. doi: 10.1016/j.phytochem.2021.112820.

Torralba, S., Raudaskoski, M., Pedregosa, A. M., and Laborda, F. (1998). Effect of cytochalasin A on apical growth, actin cytoskeleton organization and enzyme secretion in *Aspergillus nidulans*. *Microbiol. Read. Engl.* 144 (Pt 1), 45–53. doi: 10.1099/00221287-144-1-45.

Tsukada, K., Takahashi, K., and Nabeta, K. (2010). Biosynthesis of jasmonic acid in a plant pathogenic fungus, *Lasiodiplodia theobromae*. *Phytochemistry* 71, 2019–2023. doi: 10.1016/j.phytochem.2010.09.013.

Turner, T. R., James, E. K., and Poole, P. S. (2013). The plant microbiome. *Genome Biol.* 14, 209. doi: 10.1186/gb-2013-14-6-209.

Tzin, V., Galili, G., and Aharoni, A. (2012). "Shikimate pathway and aromatic amino acid biosynthesis," in *eLS*, ed.John Wiley & Sons, Ltd (Chichester, UK: John Wiley & Sons, Ltd), a0001315.pub2. doi: 10.1002/9780470015902.a0001315.pub2.

U'Ren, J. M., Lutzoni, F., Miadlikowska, J., Zimmerman, N. B., Carbone, I., May, G., et al. (2019). Host availability drives distributions of fungal endophytes in the imperilled boreal realm. *Nat. Ecol. Evol.* 3, 1430–1437. doi: 10.1038/s41559-019-0975-2.

Van Dam, N. M., and Bouwmeester, H. J. (2016). Metabolomics in the rhizosphere: tapping into belowground chemical communication. *Trends Plant Sci.* 21, 256–265. doi: 10.1016/j.tplants.2016.01.008.

Van Wees, S. C., Van der Ent, S., and Pieterse, C. M. (2008). Plant immune responses triggered by beneficial microbes. *Curr. Opin. Plant Biol.* 11, 443–448. doi: 10.1016/j.pbi.2008.05.005.

Vega, F. E., and Blackwell, M. (2005). *Insect-fungal associations: ecology and evolution*. Oxford University Press.

Vorholt, J. A., Vogel, C., Carlström, C. I., and Müller, D. B. (2017). Establishing Causality: Opportunities of Synthetic Communities for Plant Microbiome Research. *Cell Host Microbe* 22, 142–155. doi: 10.1016/j.chom.2017.07.004.

Walter, M. H., Floss, D. S., and Strack, D. (2010). Apocarotenoids: hormones, mycorrhizal metabolites and aroma volatiles. *Planta* 232, 1–17. doi: 10.1007/s00425-010-1156-3.

Wang, M., Carver, J. J., Phelan, V. V., Sanchez, L. M., Garg, N., Peng, Y., et al. (2016). Sharing and community curation of mass spectrometry data with Global Natural Products Social Molecular Networking. *Nat. Biotechnol.* 34, 828–837. doi: 10.1038/nbt.3597.

Wang, M., Schäfer, M., Li, D., Halitschke, R., Dong, C., McGale, E., et al. (2018). Blumenols as shoot markers of root symbiosis with arbuscular mycorrhizal fungi. *eLife* 7, e37093. doi: 10.7554/eLife.37093.

Wang, X., Lin, M., Xu, D., Lai, D., and Zhou, L. (2017). Structural diversity and biological activities of fungal cyclic peptides, excluding cyclodipeptides. *Mol. J. Synth. Chem. Nat. Prod. Chem.* 22, 2069. doi: 10.3390/molecules22122069.

Wani, Z. A., Ashraf, N., Mohiuddin, T., and Riyaz-Ul-Hassan, S. (2015). Plant-endophyte symbiosis, an ecological perspective. *Appl. Microbiol. Biotechnol.* 99, 2955–2965. doi: 10.1007/s00253-015-6487-3.

Wasternack, C., and Kombrink, E. (2010). Jasmonates: structural requirements for lipid-derived signals active in plant stress responses and development. *ACS Chem. Biol.* 5, 63–77. doi: DOI: 10.1021/cb900269u.

Wells, J. M., Cole, R. J., Cutler, H. C., and Spalding, D. H. (1981). *Curvularia lunata* , a new source of cytochalasin B. *Appl. Environ. Microbiol.* 41, 967–971. doi: 10.1128/aem.41.4.967-971.1981.

Wen, H., Li, Y., Liu, X., Ye, W., Yao, X., and Che, Y. (2015). Fusagerins A–F, new alkaloids from the fungus *Fusarium* sp. *Nat. Prod. Bioprospecting* 5, 195–203. doi: 10.1007/s13659-015-0067-1.

Zhang, H., Olson, D. J. H., Van, D., Purves, R. W., and Smith, M. A. (2012). Rapid identification of triacylglycerol-estolides in plant and fungal oils. *Ind. Crops Prod.* 37, 186–194. doi: 10.1016/j.indcrop.2011.10.026.

Zhang, H. W., Song, Y. C., and Tan, R. X. (2006). Biology and chemistry of endophytes. *Nat. Prod. Rep.* 23, 753–771. doi: 10.1039/b609472b.

Zhi-lin, Y., Chuan-chao, D., and Lian-qing, C. (2007). Regulation and accumulation of secondary metabolites in plant-fungus symbiotic system. *Afr. J. Biotechnol.* 6. doi: 10.4314/ajb.v6i11.57436.

Zhou, X., Zhu, H., Liu, L., Lin, J., and Tang, K. (2010). A review: recent advances and future prospects of taxol-producing endophytic fungi. *Appl. Microbiol. Biotechnol.* 86, 1707–1717. doi: 10.1007/s00253-010-2546-y.

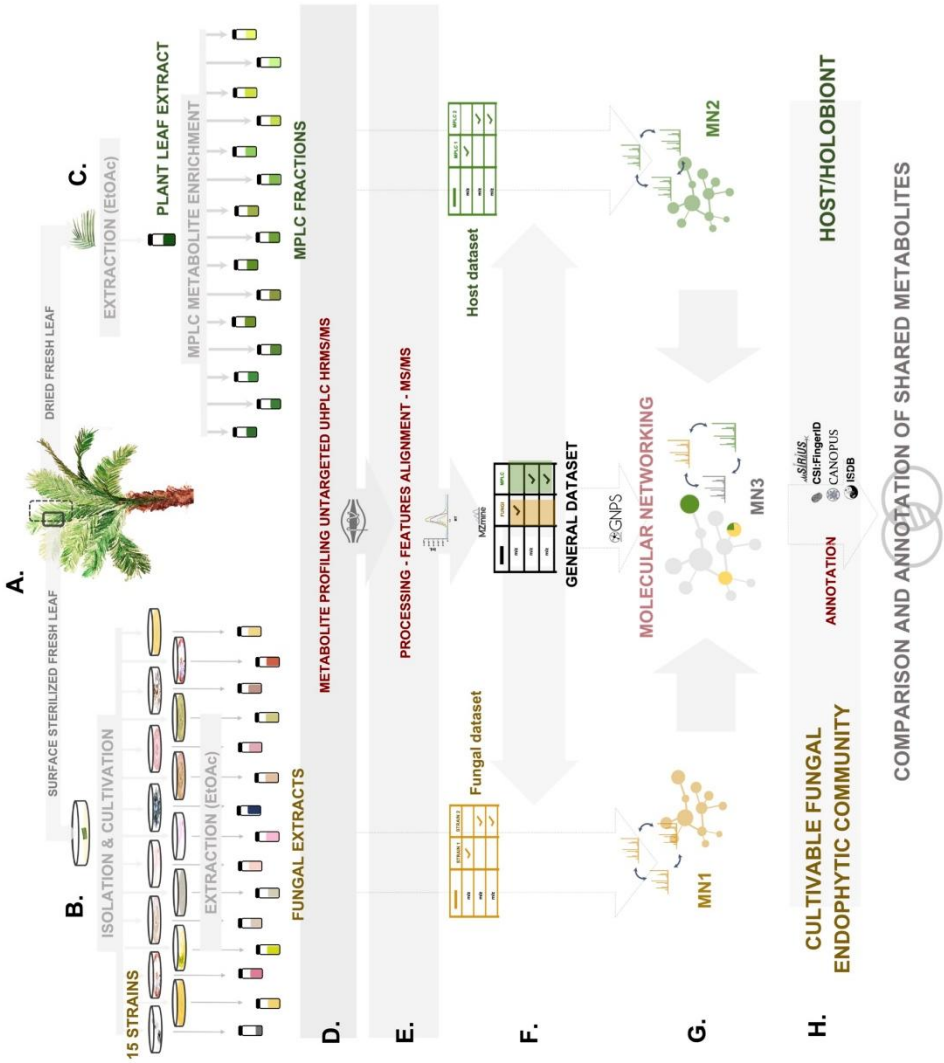

Figure 1. Experimental workflow of the study. (A) *A. sciophilum* leaf collection, (B) isolation of all cultivable fungal endophytic strains from the sterilized fresh leaf, cultivation and extraction, (C) extraction of the dried leaf and preparative MPLC fractionation for a metabolite enrichment, (D) untargeted data dependent UHPLC-HRMS/MS metabolite profiling, (E) HRMS- MS/MS data processing, (F) generation of 2 feature tables corresponding the fungal and host datasets, and creation of a common general dataset, (G) molecular networks generation for each dataset: fungal MN1, Host MN2, general MN3, (H) annotation of each datasets through a combination of spectral matching against experimental and in silico databases, as well as computational and taxonomically informed methods.

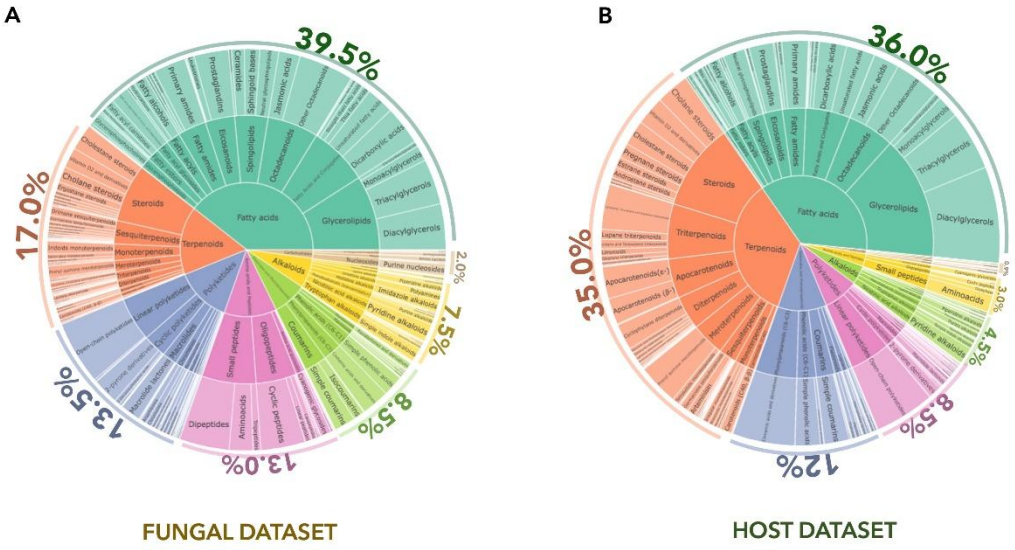

Figure 2. CANOPUS chemical annotation on the (A) fungal and (B) host datasets. Hierarchical sunburst diagrams representing the main chemical classes established using NPclassifier. The sunburst displays in the inner circle the pathway, in the middle circle the superclass and finally in the external circle, the various chemical classes. The number of associated features for each category are displayed via area size. The proportion of features annotated per chemical pathway is represented as percentages. An interactive view of the plots is available at [Interactiveplots].

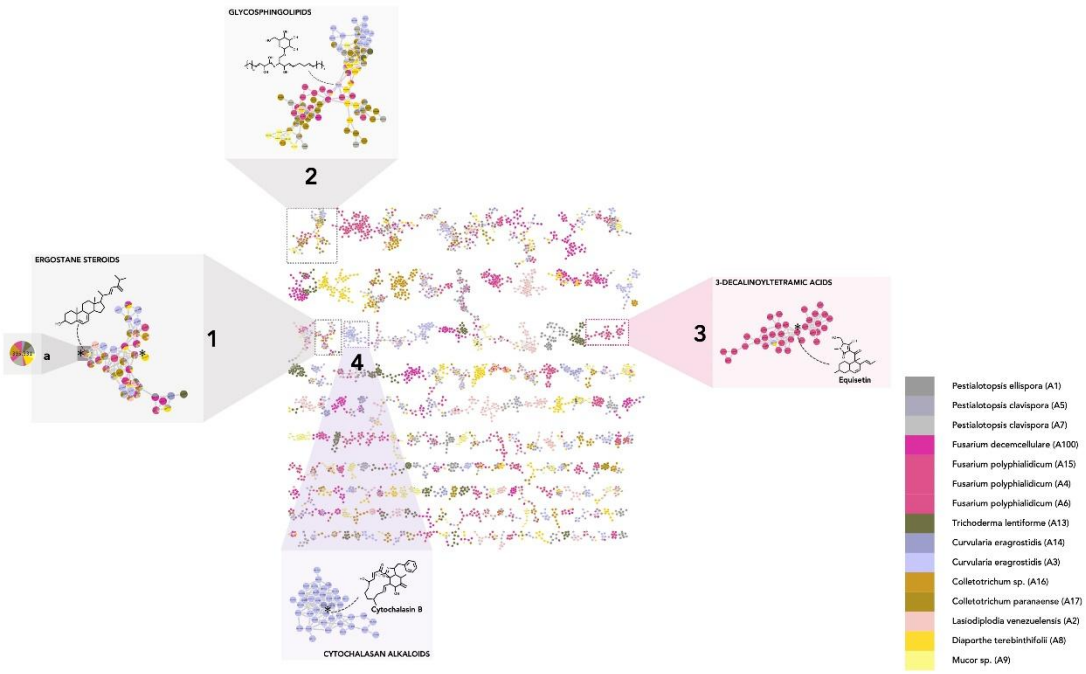

Figure 3. Molecular network on the fungal dataset (MN1). Nodes are colored based on their taxonomical attributes to denote their origin. Pie charts within each node indicate the distribution of MS intensities of each feature in the whole sample set. Nodes with single colors are characteristic for metabolites occurring only in one specific strain. Nodes with multiple colors denotes shared metabolites. (1-2) Clusters shared by multiple species, highlighting either specific shared features and/or shared chemical classes. (1a) Node corresponding to a feature detected in multiple species and annotated as 24(28)-Dehydroergosterol. (3-4) Clusters specific to particular strain(s) (single color nodes) (3: *Fusarium polyphialidicum*, 4: *Curvularia eragrostidis*).

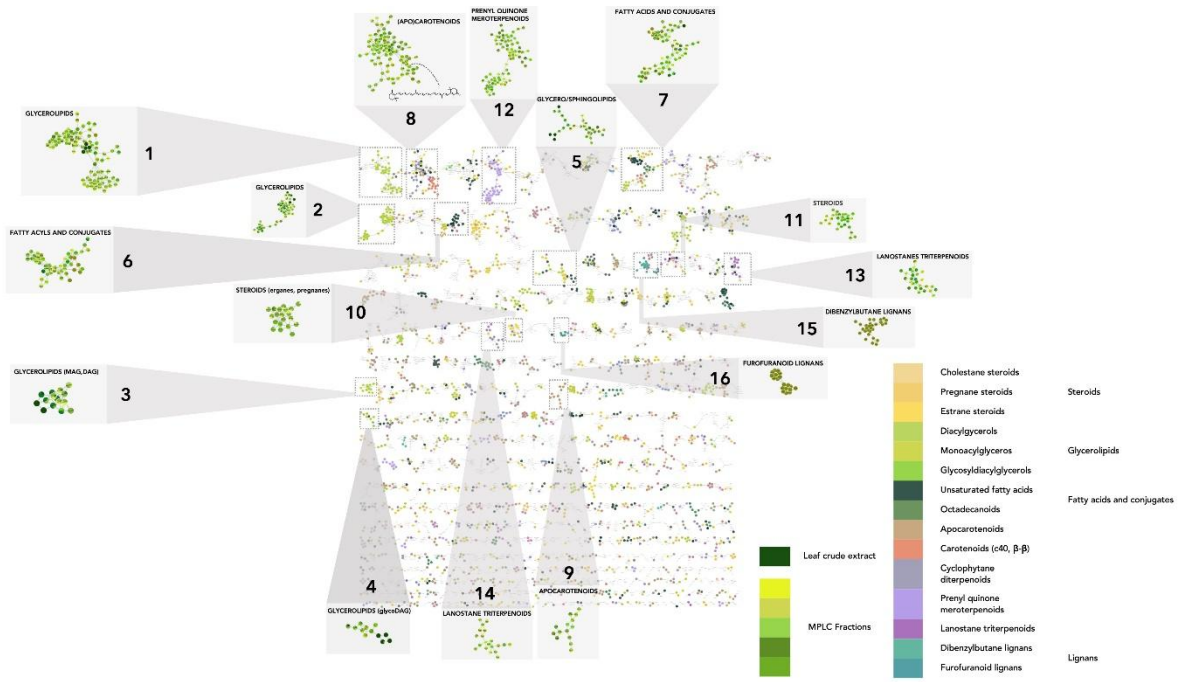

Figure 4. Molecular network on the host dataset (MN2). In the host MN, nodes are colored based on their NPclassifier chemical class. In zoomed clusters, pie charts within each node indicate the distribution of MS intensities of each feature in the leaf crude extract and/or in the MPLC fractions. (1-16) clusters of representative leaf metabolite chemical classes.

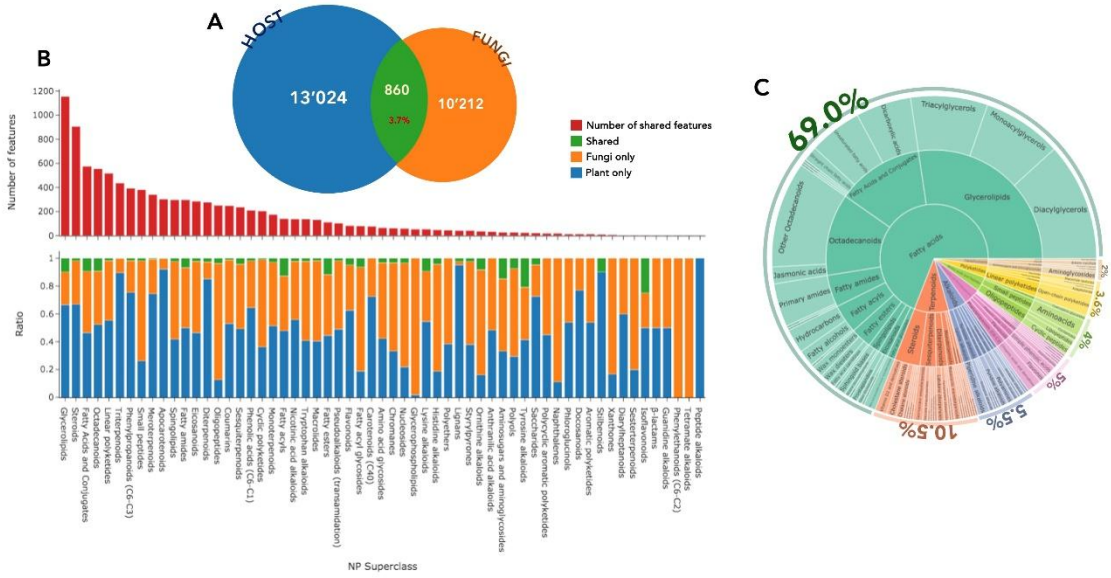

Figure 5. (A) Number of features detected in positive ion mode in the host (blue) and fungal (orange) datasets, and number of shared features (green). (B) Distribution and number (red) of these annotated features, according to the NPclassifer superclasses, in the fungal (orange), plant (blue), or shared (green) datasets. (C) Hierarchical sunburst diagram of the shared features, organized in the same way as in Fig.3. An interactive view of the plots is available at Interactiveplots.

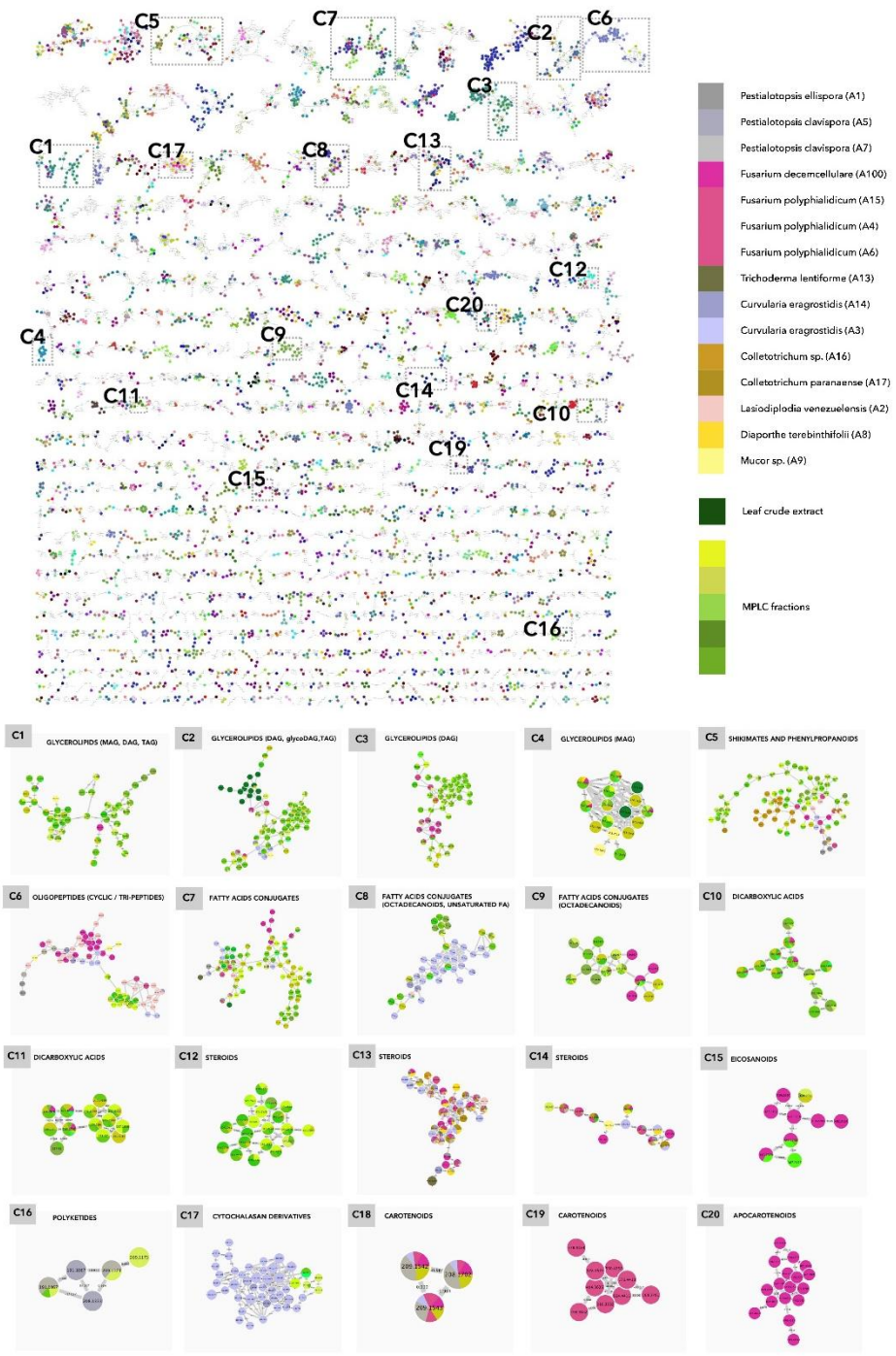

Figure 6. Molecular network of the general dataset (MN3). Nodes are colored based on their NPclassifier chemical class. In zoomed clusters, pie charts within each node indicate the distribution of MS intensities of each feature in the leaf crude extract and/or in the MPLC fractions (green colors), and/or in one or more fungal strains. (C1-C20) examples of clusters with shared features, highlighted in the MN3.

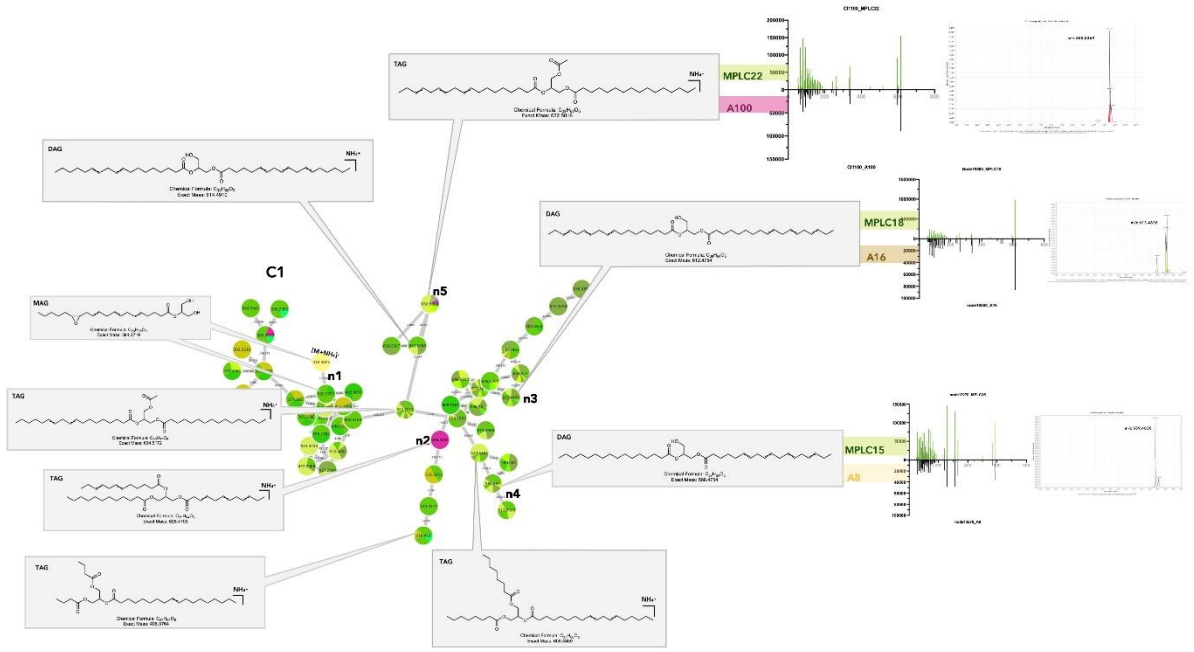

Figure 7. Selected annotations of cluster C1 from Fig.6 gathering various glycerolipids. Annotated features n3, n4, n5 are shared between the host leaf and particular strains, respectively *Colletotrichum sp.* A16, *Diaporthe terebinthifolii* A8, *Fusarium decemcellulare* A100 (for color code, see Fig. 6). n2 corresponds to a specific glycerolipid of the strain A100, detected in culture but not shared in the leaf. Representative MS/MS spectra of some annotated glycerolipids and the single ion trace of the feature across samples are displayed for shared features.

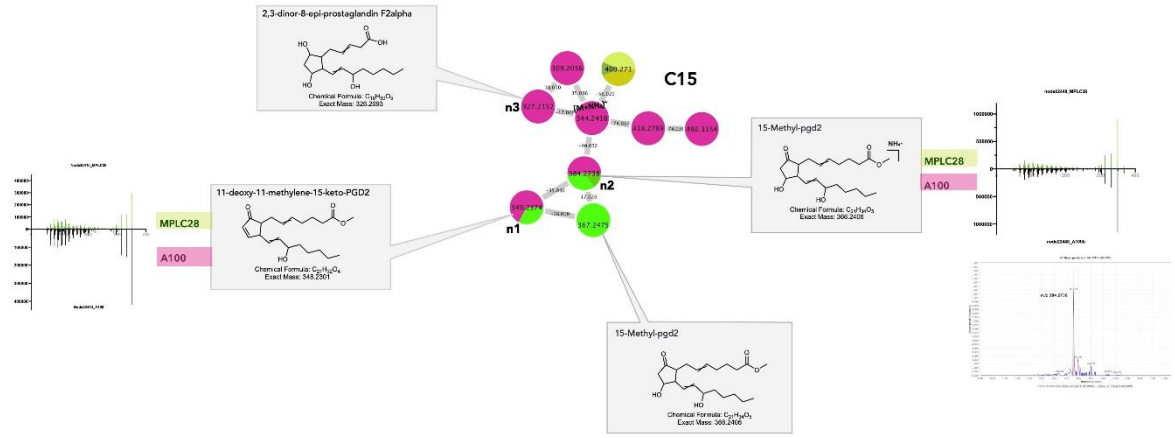

Figure 8. Selected annotations of cluster C15 from Fig.6 gathering various cyclic oxylipins. Annotated features n1, n2 are shared between the host leaf and the strain *Fusarium decemcellulare* A100 (for color code, see Fig. 6). n3 corresponds to a specific cyclic oxylipin of the strain A100, detected in culture but not shared in the leaf. *m/z* 367.2475 corresponds to a specific cyclic oxylipin from the leaf only. Representative MS/MS spectra of some

annotated cyclic oxylipins and the single ion trace of the feature across samples are displayed for shared features.

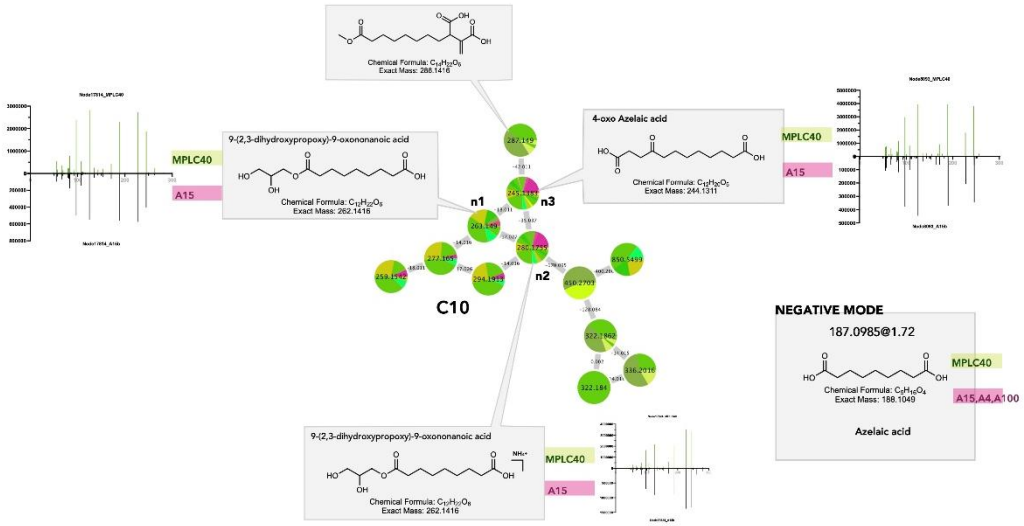

Figure 9. Selected annotations of cluster C10 from Fig.6 gathering various dicarboxylic acids. Annotated features n1, n2, n3 are shared between the host leaf and the strain *Fusarium polyphialidicum* A15 (for color code, see Fig.6). *m/z* 287.149 corresponds to a specific dicarboxylic acid from the leaf only. Azelaic acid was found as a shared metabolite evidenced in the negative ion mode dataset. Representative MS/MS spectra of some annotated dicarboxylic acids and the single ion trace of the feature across samples are displayed for shared features.

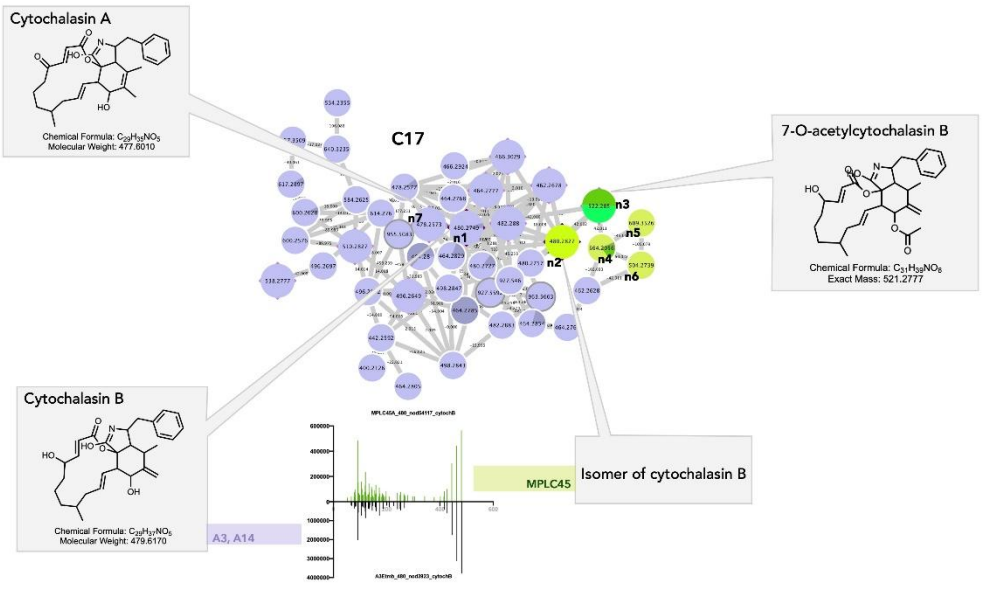

Figure 10. Selected annotations of cluster C17 from Fig.6 gathering various cytochalasin alkaloids. n7 corresponds to a specific cytochalasin alkaloid only found in the *Curvularia eragrostidis* strains A3, A14. n3 to n6 correspond to features of the leaf only annotated as cytochalasin alkaloids. n1 and n2 correspond to cytochalasin B isomers with very similar MS/MS spectra in both leaf and *Curvularia eragrostidis* strains.